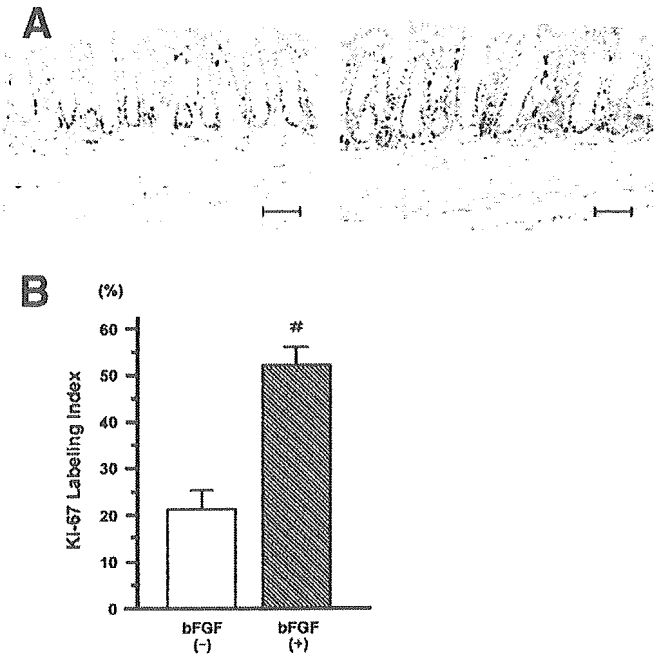

Figure 8. Immunohistochemistry of colonic tissues of normal mice using the anti–Ki-67 monoclonal antibody. (*A*) Representative histologic findings of immunohistochemical staining with anti–Ki-67 monoclonal antibody. *Left panel*, nontreated mice; *right panel*, hrbFGF-treated (5.0 mg/kg) mice. *Bars* = 100 μm. (Original magnification 200×.) (*B*) The Ki-67 labeling index. The Ki-67 labeling index was defined as the percentage of Ki-67–positive cells in the counted crypts. Five hundred nuclei in each sample were counted. Data are expressed as means ± SD (n = 3 in each group). $^{\#}P < .05$ compared with the control group.

Semiquantitative analysis of gene expression of mucosal repair-related and anti-inflammatory molecules. The gene expression of COX-2, TGF-β, ITF, and VEGF in the colonic tissues of normal mice treated with hrbFGF was significantly higher compared with nontreated normal mice (Figure 9). MUC2 mRNA expression in the colonic tissues tended to be up-regulated by treatment with hrbFGF, although there was no significant difference (Figure 9). Maximal up-regulation occurred at 6 hours (ITF), 12 hours (TGF-β, VEGF), or 24 hours (COX-2, MUC2) after hrbFGF administration. On the other hand, IL-10 and PPAR-γ mRNA expression in the colonic tissues of normal mice treated with hrbFGF was not significantly up-regulated compared with nontreated normal mice (data not shown).

Effects of hrbFGF on the Production of TGF-β in Both Epithelial and Fibroblast Cell Lines

To assess the effect of hrbFGF on TGF-β production in vitro, we measured the concentration of TGF-β in the culture media of Colon-26 or NIH3T3 cells after 24 hours of incubation with hrbFGF. In both cell lines, TGF-β production in hrbFGF-stimulated cells was significantly higher than that in nonstimulated cells (Figure 10).

Discussion

For the past 10 years, several growth factors, such as EGF, FGF, insulin-like growth factor, and hepatocyte growth factor, have been tested as potent therapeutic agents in a variety of experimental models of human IBD.[30–36] Among them, a great deal of attention has been paid to the FGF family, especially KGF-1 and KGF-2, because several clinical and experimental studies showed that they are also effective for the treatment of epithelial damage in other tissues, such as skin and oral mucosa.[37–40] Indeed, a clinical trial of KGF-2 has recently been performed for the treatment of active ulcerative colitis.[6] bFGF is also a member of the FGF family and has been shown to be effective for improving epithelial damage of several organs in animal models.[13,15–18] Based on those experimental data, human recombinant

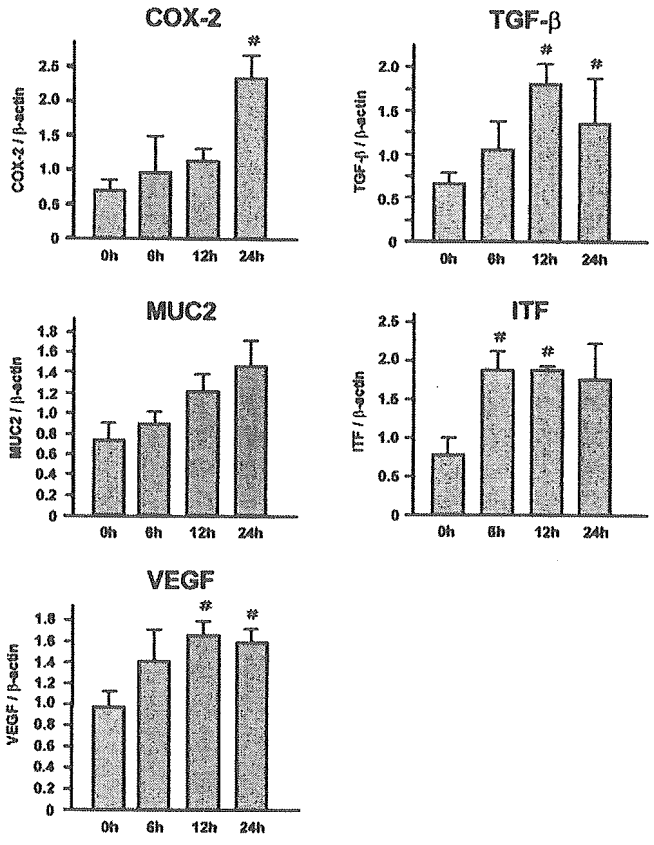

Figure 9. Effects of hrbFGF on the time-course changes of the gene expression of mucosal repair-related molecules in the colonic tissues of normal mice. The expression of each molecule RNA transcript at the indicated time periods was determined by semiquantitative reverse-transcription PCR. The results are expressed as relative ratio of each molecule to β-actin. Data are shown as means ± SD (n = 3 in each group). $^{\#}P < .05$ compared with the control group (0 hours).

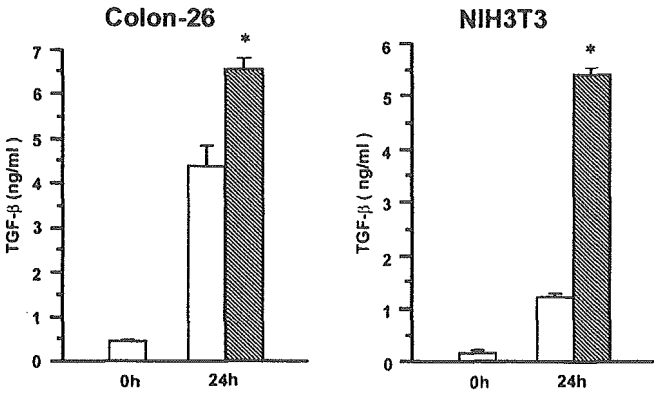

Figure 10. Effects of hrbFGF on TGF-β protein production by Colon-26 and NIH3T3 cells. Both cells were cultured for 24 hours with or without hrbFGF (100 ng/mL). The concentration of TGF-β protein was determined by enzyme-linked immunosorbent assay. *Open columns*, nonstimulated cells; *hatched columns*, hrbFGF-stimulated cells. Data are expressed as means ± SD (n = 4 in each group). $*P < .01$ compared with the conditioned media without hrbFGF.

bFGF (Trafermin; Kaken Pharmaceutical Co Ltd., Tokyo, Japan) has been clinically applied for the treatment of decubitus and dermal ulceration. However, bFGF has not yet been applied for the treatment of human IBD.

In this study, we first showed that rectal administration of hrbFGF had therapeutic effects in a DSS-induced colitis model. Indeed, hrbFGF recovered the decrease in body weight and histologically improved colitis. In our study, we confirmed that bFGF treatment did not yet improve DSS-induced colitis on day 8 (data not shown). In contrast, histologic analysis on day 11 revealed a significant improvement of DSS-induced colitis by bFGF treatment. Therefore, we consider that bFGF enhanced wound repair in the colonic tissues of mice with DSS-induced colitis rather than protected the colon against DSS-induced injury in this study.

In our preliminary study, intraperitoneal injection of hrbFGF (5.0 mg · kg^{-1} · day^{-1}) significantly improved body weight loss and colonic injury in a DSS-induced colitis model (data not shown). However, bFGF is considered to be rapidly cleared from the circulation, because the serum half-life of bFGF is reported to be 1.5–50 minutes after intravenous administration.[41–43] In addition, it was recently reported that rectal administration of EGF is effective for patients with active ulcerative colitis.[7] Moreover, systemic administration of bFGF might cause adverse effects, because bFGF mediates its biologic effects by binding to a variety of high-affinity cell-surface receptors, which are distributed not only in the colonic mucosa but also throughout the body.[44] Therefore, we considered that topical administration of bFGF might be more effective and less hazardous for the treatment of IBD than systemic administration, directly delivering bFGF to injured colonic mucosa.

Several mechanisms are considered for the improvement of colonic injury by bFGF. bFGF has been shown to stimulate proliferation of several intestinal cell lines.[22] We showed in this study that bFGF significantly increased the number of Ki-67–positive cells in the colonic epithelium of normal mice at 24 hours after bFGF treatment. Previous studies have shown that the increase of Ki-67–positive cell numbers directly correlates with crypt cell proliferation in the intestinal mucosa.[45–47] Interestingly, it was recently reported that exogenous bFGF markedly enhanced crypt stem cell survival in the mouse after radiation injury.[23] Vidrich reported that FGF receptor-3, whose ligand includes bFGF, was expressed prominently in the epithelial stem cell compartment.[48] Taken together, bFGF might enhance epithelial cell proliferation primarily through its direct effect on intestinal epithelial cells, including stem cells.

The present study clearly showed that TGF-β mRNA expression in the colonic tissues of normal mice was up-regulated after administration of bFGF. Moreover, we confirmed by enzyme-linked immunosorbent assay that bFGF increased TGF-β production in not only colonic epithelial cell lines but also fibroblast cell lines. Using an in vitro wounding model, Ciacci et al reported that TGF-β promotes cell migration, which does not require cell proliferation.[49] Moreover, Dignass et al showed that bFGF enhanced epithelial cell restitution through a TGF-β–dependent pathway in vitro.[22] In addition to cell proliferation, epithelial restitution is also known to play a significant role in the repair process of epithelial injury in the gastrointestinal tract.[3,4] Accordingly, TGF-β might be involved in the improvement of DSS-induced colitis by bFGF treatment through the enhancement of epithelial restitution. However, it may be noted that TGF-β is known to inhibit cell proliferation in epithelial cells. Thus, bFGF-induced TGF-β production also may be important in inhibiting unrestrained cell proliferation, as suggested previously.[22,50] Furthermore, because TGF-β is known to inhibit the production of proinflammatory cytokines, such as TNF-α and interferon gamma, in activated immune cells,[51] TGF-β may also have a role in down-regulation of inflammatory responses in DSS-induced colitis.

In this study, MUC2 and ITF gene expression in the colonic tissue of normal mice was up-regulated by treatment with bFGF. Moreover, the decreased mRNA expression of MUC2 and ITF in the colonic tissues of mice with DSS-induced colitis was recovered or even enhanced by bFGF treatment. Both MUC2 and ITF are predominantly expressed in the goblet cells of the small and large intestine.[52,53] Thus, the increase of MUC2 and ITF mRNA expression in the colonic tissues of mice with

DSS-induced colitis by bFGF treatment may have resulted from not only the direct effect of bFGF on those gene expressions but also recovery of goblet cell numbers. MUC2 is one of the secreted mucins and forms a gel-like mucus layer, which serves as a barrier to protect the intestinal epithelium from injurious luminal stimulants.[53] ITF promotes epithelial restitution after injury through epithelial cell migration.[54] Furthermore, several lines of evidence suggest that trefoil factors are involved in the stabilization of the mucus layer.[55,56] Taken together, it might be that bFGF has a role in enhancing mucosal barrier function not only by restoring injured epithelial structures but also by promoting mucus secretion and/or stabilization.

It may be noted in our study that although bFGF administration significantly reduced COX-2 gene expression in the colonic tissue of mice with DSS-induced colitis, it significantly enhanced COX-2 gene expression in normal colonic tissue. COX-2 is one of the key molecules involved in the mucosal repair process. Indeed, it has been shown that COX-2–mediated prostaglandin production contributes to the protection of colonic injury, the increase in crypt stem cell survival, the enhancement of angiogenesis, and the inhibition of proinflammatory cytokine production by activated macrophages.[57–62] Recently, Tessner et al reported that bFGF up-regulates COX-2 in human intestinal cell line I407,[63] and we obtained a similar stimulatory effect of bFGF on human colonic epithelial cell line Caco-2 (data not shown). Moreover, bFGF up-regulates COX-2 expression in endothelial cells, and COX-2 enhances bFGF-induced angiogenesis by stimulating VEGF gene expression.[64,65] In support of those data, the present study showed that hrbFGF significantly enhanced VEGF mRNA expression in the colonic tissues of normal mice. Taken together, therefore, bFGF appears to have a direct stimulatory action on COX-2 gene expression, which might result in the acceleration of mucosal repair in part through the induction of angiogenesis. However, our data also showed that gene expression of COX-2 and VEGF in the mice with hrbFGF-treated colitis was lower than in the nontreated mice with colitis in a dose-dependent manner. These discordant results were probably due to reduced inflammation in the colonic tissues of mice with DSS-induced colitis by the treatment with hrbFGF.

Zhao et al previously reported that costimulation with acidic FGF and anti-CD3 antibody activated $CD4^+$ T cells in vitro[66] and suggested an inflammatory effect of bFGF. In the present study, however, we did not find significant differences in the number of $CD4^+$ T cells or $CD4^+CD69^+$ T cells from MLN between mice with DSS-induced colitis with and without bFGF treatment. Moreover, the gene expression of anti-inflammatory molecules, such as IL-10 and PPAR-γ, in the colonic tissues of normal mice treated with bFGF was not influenced (data not shown). Thus, neither the number nor the function of immune-regulatory cells seemed to be affected by bFGF administration in our study.

In this study, we also examined the efficacy of bFGF on TNBS-induced colitis, a typical model of T cell–mediated colitis. Histologic analysis revealed that regeneration of colonic epithelium was enhanced by bFGF treatment, although bFGF treatment did not reduce lymphocytic infiltration in the colonic tissues of mice with TNBS-induced colitis. Additionally, the survival rate in the hrbFGF-treated group was significantly higher than in the nontreated group. Thus, bFGF could accelerate mucosal healing even in TNBS-induced colitis, mainly by promoting epithelial cell growth but not by exerting a direct anti-inflammatory effect on T cells.

In summary, our study suggests that rectal administration of bFGF is a promising option for the treatment of IBD. The safety of bFGF is already established because bFGF has been clinically applied to human diseases. A novel approach using bFGF might exert a synergistic effect with immune-regulatory agents for the treatment of IBD.

References

1. Fiocchi C. Inflammatory bowel disease: etiology and pathogenesis. Gastroenterology 1998;115:182–205.
2. Sartor RB. Intestinal microflora in human and experimental inflammation bowel disease. Curr Opin Gastroenterol 2001;17:324–330.
3. Goke M, Podolsky DK. Regulation of the mucosal epithelial barrier. Baillieres Clin Gastroenterol 1996;10:393–405.
4. Dignass AU. Mechanisms and modulation of intestinal epithelial repair. Inflamm Bowel Dis 2001;7:68–77.
5. Dignass AU, Sturm A. Peptide growth factors in the intestine. Eur J Gastroenterol Hepatol 2001;13:763–770.
6. Sandborn WJ, Sands BE, Wolf DC, Valentine JF, Safdi M, Katz S, Isaacs KL, Wruble LD, Katz J, Present DH, Loftus EV Jr, Graeme-Cook F, Odenheimer DJ, Hanauer SB. Repifermin (keratinocyte growth factor-2) for the treatment of active ulcerative colitis: a randomized, double-blind, placebo-controlled, dose-escalation trial. Aliment Pharmacol Ther 2003;17:1355–1364.
7. Sinha A, Nightingale J, West KP, Berlanga-Acosta J, Playford RJ. Epidermal growth factor enemas with oral mesalamine for mild-to-moderate left-sided ulcerative colitis or proctitis. N Engl J Med 2003;349:350–357.
8. Basilico C, Moscatelli D. The FGF family of growth factors and oncogenes. Adv Cancer Res 1992;59:115–165.
9. Schwartz SM, Liaw L. Growth control and morphogenesis in the development and pathology of arteries. J Cardiovasc Pharmacol 1993;21(Suppl 1):S31–S49.
10. Yanagisawa-Miwa A, Uchida Y, Nakamura F, Tomaru T, Kido H, Kamijo T, Sugimoto T, Kaji K, Utsuyama M, Kurashima C, et al. Salvage of infarcted myocardium by angiogenic action of basic fibroblast growth factor. Science 1992;257:1401–1403.
11. Harada K, Grossman W, Friedman M, Edelman ER, Prasad PV, Keighley CS, Manning WJ, Sellke FW, Simons M. Basic fibroblast

growth factor improves myocardial function in chronically ischemic porcine hearts. J Clin Invest 1994;94:623–630.
12. Bikfalvi A, Klein S, Pintucci G, Rifkin DB. Biological roles of fibroblast growth factor-2. Endocr Rev 1997;18:26–45.
13. Rieck P, Assouline M, Hartmann C, Pouliquen Y, Courtois Y. [Effect of recombinant human basic fibroblast growth factor (rh-bFGF) on wound healing of the corneal epithelium]. Ophthalmologe 1993;90:646–651.
14. Hoppenreijs VP, Pels E, Vrensen GF, Treffers WF. Basic fibroblast growth factor stimulates corneal endothelial cell growth and endothelial wound healing of human corneas. Invest Ophthalmol Vis Sci 1994;35:931–944.
15. Schuschereba ST, Bowman PD, Ferrando RE, Lund DJ, Quong JA, Vargas JA. Accelerated healing of laser-injured rabbit retina by basic fibroblast growth factor. Invest Ophthalmol Vis Sci 1994; 35:945–954.
16. Stenberg BD, Phillips LG, Hokanson JA, Heggers JP, Robson MC. Effect of bFGF on the inhibition of contraction caused by bacteria. J Surg Res 1991;50:47–50.
17. LeGrand EK, Burke JF, Costa DE, Kiorpes TC. Dose responsive effects of PDGF-BB, PDGF-AA, EGF, and bFGF on granulation tissue in a guinea pig partial thickness skin excision model. Growth Factors 1993;8:307–314.
18. Albertson S, Hummel RP III, Breeden M, Greenhalgh DG. PDGF and FGF reverse the healing impairment in protein-malnourished diabetic mice. Surgery 1993;114:368–372; discussion 372–373.
19. Nozaki K, Finklestein SP, Beal MF. Basic fibroblast growth factor protects against hypoxia-ischemia and NMDA neurotoxicity in neonatal rats. J Cereb Blood Flow Metab 1993;13:221–228.
20. Logan A, Berry M. Transforming growth factor-beta 1 and basic fibroblast growth factor in the injured CNS. Trends Pharmacol Sci 1993;14:337–342.
21. Ortega S, Ittmann M, Tsang SH, Ehrlich M, Basilico C. Neuronal defects and delayed wound healing in mice lacking fibroblast growth factor 2. Proc Natl Acad Sci U S A 1998;95:5672–5677.
22. Dignass AU, Tsunekawa S, Podolsky DK. Fibroblast growth factors modulate intestinal epithelial cell growth and migration. Gastroenterology 1994;106:1254–1262.
23. Houchen CW, George RJ, Sturmoski MA, Cohn SM. FGF-2 enhances intestinal stem cell survival and its expression is induced after radiation injury. Am J Physiol 1999;276:G249–G258.
24. Okayasu I, Hatakeyama S, Yamada M, Ohkusa T, Inagaki Y, Nakaya R. A novel method in the induction of reliable experimental acute and chronic ulcerative colitis in mice. Gastroenterology 1990;98:694–702.
25. Williams KL, Fuller CR, Dieleman LA, DaCosta CM, Haldeman KM, Sartor RB, Lund PK. Enhanced survival and mucosal repair after dextran sodium sulfate-induced colitis in transgenic mice that overexpress growth hormone. Gastroenterology 2001;120: 925–937.
26. Gibson UE, Heid CA, Williams PM. A novel method for real time quantitative RT-PCR. Genome Res 1996;6:995–1001.
27. Winer J, Jung CK, Shackel I, Williams PM. Development and validation of real-time quantitative reverse transcriptase-polymerase chain reaction for monitoring gene expression in cardiac myocytes in vitro. Anal Biochem 1999;270:41–49.
28. Neurath MF, Fuss I, Kelsall BL, Stuber E, Strober W. Antibodies to interleukin 12 abrogate established experimental colitis in mice. J Exp Med 1995;182:1281–1290.
29. Elson CO, Beagley KW, Sharmanov AT, Fujihashi K, Kiyono H, Tennyson GS, Cong Y, Black CA, Ridwan BW, McGhee JR. Hapten-induced model of murine inflammatory bowel disease: mucosa immune responses and protection by tolerance. J Immunol 1996;157:2174–2185.
30. Luck MS, Bass P. Effect of epidermal growth factor on experimental colitis in the rat. J Pharmacol Exp Ther 1993;264:984–990.
31. Procaccino F, Reinshagen M, Hoffmann P, Zeeh JM, Lakshmanan J, McRoberts JA, Patel A, French S, Eysselein VE. Protective effect of epidermal growth factor in an experimental model of colitis in rats. Gastroenterology 1994;107:12–17.
32. Egger B, Procaccino F, Sarosi I, Tolmos J, Buchler MW, Eysselein VE. Keratinocyte growth factor ameliorates dextran sodium sulfate colitis in mice. Dig Dis Sci 1999;44:836–844.
33. Byrne FR, Farrell CL, Aranda R, Rex KL, Scully S, Brown HL, Flores SA, Gu LH, Danilenko DM, Lacey DL, Ziegler TR, Senaldi G. rHuKGF ameliorates symptoms in DSS and CD4(+)CD45RB(Hi) T cell transfer mouse models of inflammatory bowel disease. Am J Physiol Gastrointest Liver Physiol 2002;282:G690–G701.
34. Miceli R, Hubert M, Santiago G, Yao DL, Coleman TA, Huddleston KA, Connolly K. Efficacy of keratinocyte growth factor-2 in dextran sulfate sodium-induced murine colitis. J Pharmacol Exp Ther 1999;290:464–471.
35. Han DS, Li F, Holt L, Connolly K, Hubert M, Miceli R, Okoye Z, Santiago G, Windle K, Wong E, Sartor RB. Keratinocyte growth factor-2 (FGF-10) promotes healing of experimental small intestinal ulceration in rats. Am J Physiol Gastrointest Liver Physiol 2000;279:G1011–G1022.
36. Jeffers M, McDonald WF, Chillakuru RA, Yang M, Nakase H, Deegler LL, Sylander ED, Rittman B, Bendele A, Sartor RB, Lichenstein HS. A novel human fibroblast growth factor treats experimental intestinal inflammation. Gastroenterology 2002;123:1151–1162.
37. Farrell CL, Rex KL, Chen JN, Bready JV, DiPalma CR, Kaufman SA, Rattan A, Scully S, Lacey DL. The effects of keratinocyte growth factor in preclinical models of mucositis. Cell Prolif 2002; 35(Suppl 1):78–85.
38. Meropol NJ, Somer RA, Gutheil J, Pelley RJ, Modiano MR, Rowinsky EK, Rothenberg ML, Redding SW, Serdar CM, Yao B, Heard R, Rosen LS. Randomized phase I trial of recombinant human keratinocyte growth factor plus chemotherapy: potential role as mucosal protectant. J Clin Oncol 2003;21:1452–1458.
39. Jimenez PA, Rampy MA. Keratinocyte growth factor-2 accelerates wound healing in incisional wounds. J Surg Res 1999;81:238–242.
40. Robson MC, Phillips TJ, Falanga V, Odenheimer DJ, Parish LC, Jensen JL, Steed DL. Randomized trial of topically applied repifermin (recombinant human keratinocyte growth factor-2) to accelerate wound healing in venous ulcers. Wound Repair Regen 2001;9:347–352.
41. Whalen GF, Shing Y, Folkman J. The fate of intravenously administered bFGF and the effect of heparin. Growth Factors 1989;1: 157–164.
42. Edelman ER, Nugent MA, Karnovsky MJ. Perivascular and intravenous administration of basic fibroblast growth factor: vascular and solid organ deposition. Proc Natl Acad Sci U S A 1993;90: 1513–1517.
43. Lazarous DF, Shou M, Stiber JA, Dadhania DM, Thirumurti V, Hodge E, Unger EF. Pharmacodynamics of basic fibroblast growth factor: route of administration determines myocardial and systemic distribution. Cardiovasc Res 1997;36:78–85.
44. Hughes SE. Differential expression of the fibroblast growth factor receptor (FGFR) multigene family in normal human adult tissues. J Histochem Cytochem 1997;45:1005–1019.
45. Gerdes J, Schwab U, Lemke H, Stein H. Production of a mouse monoclonal antibody reactive with a human nuclear antigen associated with cell proliferation. Int J Cancer 1983;31:13–20.
46. Johnston PG, O'Brien MJ, Dervan PA, Carney DN. Immunohistochemical analysis of cell kinetic parameters in colonic adenocarcinomas, adenomas, and normal mucosa. Hum Pathol 1989;20: 696–700.

47. Gerdes J, Lemke H, Baisch H, Wacker HH, Schwab U, Stein H. Cell cycle analysis of a cell proliferation-associated human nuclear antigen defined by the monoclonal antibody Ki-67. J Immunol 1984;133:1710–1715.
48. Vidrich A. Signaling through FGFR3 is neccesary for expansion of the epithelial stem cell compartment during normal intestinal development (abstr). Gastroenterology 2003;124:A22.
49. Ciacci C, Lind SE, Podolsky DK. Transforming growth factor beta regulation of migration in wounded rat intestinal epithelial monolayers. Gastroenterology 1993;105:93–101.
50. Suemori S, Ciacci C, Podolsky DK. Regulation of transforming growth factor expression in rat intestinal epithelial cell lines. J Clin Invest 1991;87:2216–2221.
51. Letterio JJ, Roberts AB. Regulation of immune responses by TGF-beta. Annu Rev Immunol 1998;16:137–161.
52. Wong WM, Poulsom R, Wright NA. Trefoil peptides. Gut 1999; 44:890–895.
53. Corfield AP, Myerscough N, Longman R, Sylvester P, Arul S, Pignatelli M. Mucins and mucosal protection in the gastrointestinal tract: new prospects for mucins in the pathology of gastrointestinal disease. Gut 2000;47:589–594.
54. Dignass A, Lynch-Devaney K, Kindon H, Thim L, Podolsky DK. Trefoil peptides promote epithelial migration through a transforming growth factor beta-independent pathway. J Clin Invest 1994; 94:376–383.
55. Kindon H, Pothoulakis C, Thim L, Lynch-Devaney K, Podolsky DK. Trefoil peptide protection of intestinal epithelial barrier function: cooperative interaction with mucin glycoprotein. Gastroenterology 1995;109:516–523.
56. Sands BE, Podolsky DK. The trefoil peptide family. Annu Rev Physiol 1996;58:253–273.
57. Tessner TG, Cohn SM, Schloemann S, Stenson WF. Prostaglandins prevent decreased epithelial cell proliferation associated with dextran sodium sulfate injury in mice. Gastroenterology 1998;115:874–882.
58. Morteau O, Morham SG, Sellon R, Dieleman LA, Langenbach R, Smithies O, Sartor RB. Impaired mucosal defense to acute colonic injury in mice lacking cyclooxygenase-1 or cyclooxygenase-2. J Clin Invest 2000;105:469–478.
59. Form DM, Auerbach R. PGE2 and angiogenesis. Proc Soc Exp Biol Med 1983;172:214–218.
60. Cohn SM, Schloemann S, Tessner T, Seibert K, Stenson WF. Crypt stem cell survival in the mouse intestinal epithelium is regulated by prostaglandins synthesized through cyclooxygenase-1. J Clin Invest 1997;99:1367–1379.
61. Knudsen PJ, Dinarello CA, Strom TB. Prostaglandins posttranscriptionally inhibit monocyte expression of interleukin 1 activity by increasing intracellular cyclic adenosine monophosphate. J Immunol 1986;137:3189–3194.
62. Marcinkiewicz J. In vitro cytokine release by activated murine peritoneal macrophages: role of prostaglandins in the differential regulation of tumor necrosis factor alpha, interleukin 1, and interleukin 6. Cytokine 1991;3:327–332.
63. Tessner TG, Muhale F, Schloemann S, Cohn SM, Morrison A, Stenson WF. Basic fibroblast growth factor upregulates cyclooxygenase-2 in I407 cells through p38 MAP kinase. Am J Physiol Gastrointest Liver Physiol 2003;284:G269–G279.
64. Kage K, Fujita N, Oh-hara T, Ogata E, Fujita T, Tsuruo T. Basic fibroblast growth factor induces cyclooxygenase-2 expression in endothelial cells derived from bone. Biochem Biophys Res Commun 1999;254:259–263.
65. Majima M, Hayashi I, Muramatsu M, Katada J, Yamashina S, Katori M. Cyclo-oxygenase-2 enhances basic fibroblast growth factor-induced angiogenesis through induction of vascular endothelial growth factor in rat sponge implants. Br J Pharmacol 2000;130:641–649.
66. Zhao XM, Byrd VM, McKeehan WL, Reich MB, Miller GG, Thomas JW. Costimulation of human CD4+ T cells by fibroblast growth factor-1 (acidic fibroblast growth factor). J Immunol 1995;155: 3904–3911.

Received March 15, 2004. Accepted December 22, 2004.

Address requests for reprints to: Kazuichi Okazaki, MD, PhD, Third Department of Internal Medicine, Kansai Medical University, 10-15 Fumizono-cho, Moriguchi City, Osaka, 570-8506, Japan. e-mail: okazaki@takii.kmu.ac.jp; fax: (81) 6-6996-4874.

Supported in part by the Establishment of International COE for Integration of Transplantation Therapy and Regenerative Medicine (COE program of the Ministry of Education, Culture, Sports, Science, and Technology, Japan); Grant-in-Aid for Scientific Research (C) from the Ministry of Culture and Science in Japan (16560645); and Health and Labour Science Research Grants from the Japanese Ministry of Health, Labour and Welfare, and Research on Measures for Intractable Disease (Inflammatory Bowel Disease).

Immunity 24, 41–51, January 2006 ©2006 Elsevier Inc. DOI 10.1016/j.immuni.2005.11.004

IκBNS Inhibits Induction of a Subset of Toll-like Receptor-Dependent Genes and Limits Inflammation

Hirotaka Kuwata,[1] Makoto Matsumoto,[1] Koji Atarashi,[1] Hideaki Morishita,[1] Tomohiro Hirotani,[2] Ritsuko Koga,[1] and Kiyoshi Takeda[1,*]
[1] Department of Molecular Genetics
Medical Institute of Bioregulation
Kyushu University
3-1-1 Maidashi, Higashi-ku
Fukuoka 812-8582
Japan
[2] Department of Gastroenterology and Hepatology
Graduate School of Medicine
Osaka University
2-2 Yamada-oka, Suita
Osaka 565-0871
Japan

Summary

Toll-like receptor (TLR)-mediated immune responses are downregulated by several mechanisms that affect signaling pathways. However, it remains elusive how TLR-mediated gene expression is differentially modulated. Here, we show that IκBNS, a TLR-inducible nuclear IκB protein, negatively regulates induction of a subset of TLR-dependent genes through inhibition of NF-κB activity. IκBNS-deficient macrophages and dendritic cells show increased TLR-mediated expression of genes such as IL-6 and IL-12p40, which are induced late after TLR stimulation. In contrast, IκBNS-deficient cells showed normal induction of genes that are induced early or induced via IRF-3 activation. LPS stimulation of IκBNS-deficient macrophages prolonged NF-κB activity at the specific promoters, indicating that IκBNS mediates termination of NF-κB activity at selective gene promoters. Moreover, IκBNS-deficient mice are highly susceptible to LPS-induced endotoxin shock and intestinal inflammation. Thus, IκBNS regulates inflammatory responses by inhibiting the induction of a subset of TLR-dependent genes through modulation of NF-κB activity.

Introduction

Toll-like receptors (TLRs) are implicated in the recognition of specific patterns of microbial components and subsequent induction of gene expression. TLR-dependent gene expression is induced through activation of two distinct signaling pathways mediated by the Toll/IL-1 receptor (TIR) domain-containing adaptors MyD88 and TRIF. These signaling pathways finally culminate in the activation of several transcription factors, such as NF-κB and IRF families (Akira and Takeda, 2004). The MyD88-dependent gene induction is achieved by an early phase of NF-κB and IRF-5 activation in macrophages (Kawai et al., 1999; Takaoka et al., 2005). The TRIF-dependent gene induction is mainly regulated by IRF-3 (Sakaguchi et al., 2003; Yamamoto et al., 2003).

TLR-mediated gene expression regulates activation of not only innate immunity but also adaptive immunity, which provides antigen-specific responses against harmful pathogens (Iwasaki and Medzhitov, 2004; Pasare and Medzhitov, 2004). However, TLR-mediated activation of innate immunity, when in excess, triggers development of autoimmune disorders and inflammatory diseases, such as SLE, cardiomyopathy, atherosclerosis, diabetes mellitus, and inflammatory bowel diseases (Bjorkbacka et al., 2004; Eriksson et al., 2003; Kobayashi et al., 2003; Lang et al., 2005; Leadbetter et al., 2002; Michelsen et al., 2004). Excessive activation of TLR4 by LPS induces endotoxin shock, a serious systemic disorder with a high mortality rate. Therefore, TLR-dependent innate immune responses must be finely regulated, and underlying mechanisms are now being examined extensively (Liew et al., 2005). Several negative regulators of TLR-mediated signaling pathways have been proposed. Cytoplasmic molecules, such as an alternatively spliced short form of MyD88 (MyD88s), IRAK-M, SOCS1, A20, PI3-kinase, and TRIAD3A, are all involved in negative regulation of TLR pathways (Boone et al., 2004; Burns et al., 2003; Chuang and Ulevitch, 2004; Fukao et al., 2002; Kinjyo et al., 2002; Kobayashi et al., 2002; Nakagawa et al., 2002). Membrane bound SIGIRR, ST2, TRAILR, and RP105 are also implicated in these processes (Brint et al., 2004; Diehl et al., 2004; Divanovic et al., 2005; Wald et al., 2003).

TLR-dependent gene induction is also regulated by nuclear IκB proteins, such as IκBζ, Bcl-3, and IκBNS. IκBζ is indispensable for positive regulation of a subset of TLR-dependent genes, such as IL-6 and IL-12p40 (Yamamoto et al., 2004). In contrast, Bcl-3 and IκBNS seem to be involved in negative regulation of TLR-dependent gene induction. Bcl-3 was shown to be involved in selective inhibition of TLR-dependent TNF-α production (Kuwata et al., 2003; Wessells et al., 2004). An in vitro study indicated that IκBNS is induced by IL-10 or LPS and selectively inhibits IL-6 production in macrophages (Hirotani et al., 2005). Thus, nuclear IκB proteins differentially regulate TLR-dependent gene expression. However, the physiological role of IκBNS is still unclear.

In this study, we analyzed TLR-dependent inflammatory responses in IκBNS-deficient mice. We found that IκBNS is involved in selective inhibition of a subset of MyD88-dependent genes, including IL-6, IL-12p40, and IL-18. In IκBNS-deficient macrophages, LPS-induced activation of NF-κB was prolonged. Accordingly, IκBNS-deficient mice showed increased production of these cytokines accompanied by high sensitivity to LPS-induced endotoxin shock. Furthermore, IκBNS-deficient mice were highly susceptible to intestinal inflammation caused by disruption of the epithelial barrier. These findings indicate that IκBNS inhibits the induction of a group of TLR-dependent genes, thereby preventing excessive inflammation.

*Correspondence: ktakeda@bioreg.kyushu-u.ac.jp

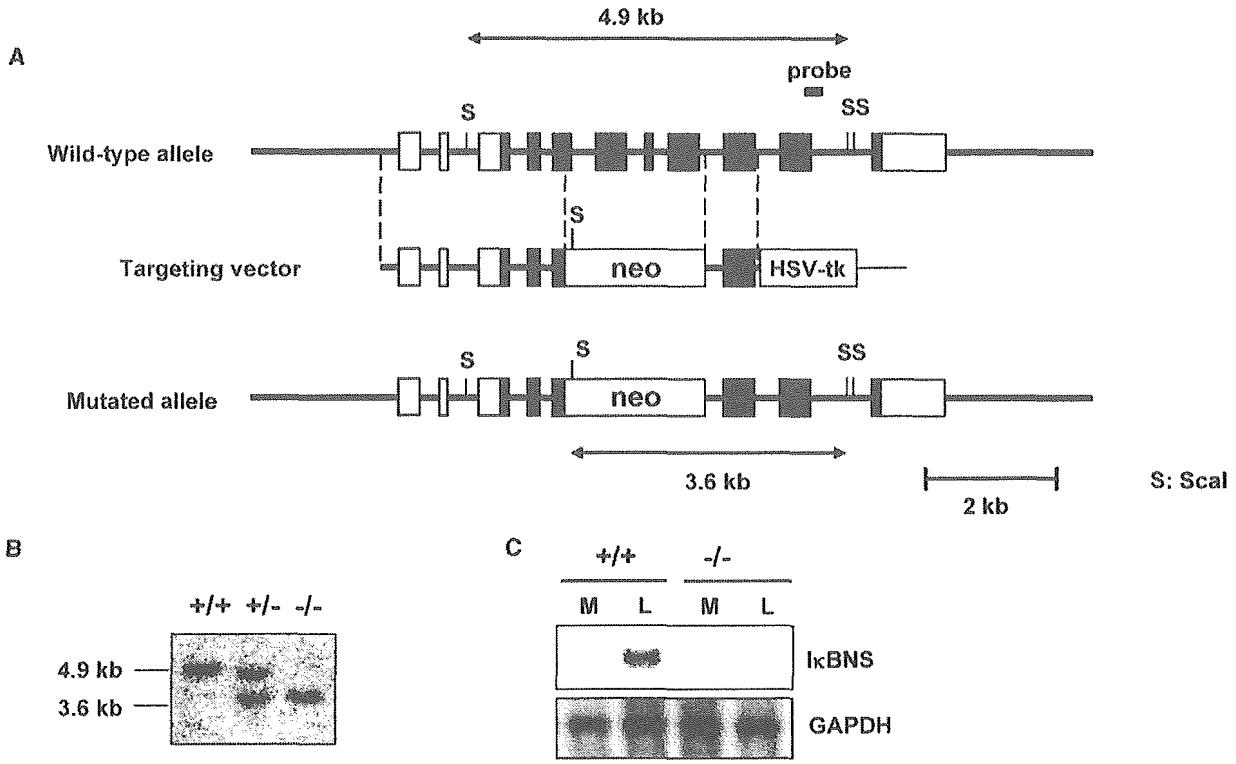

Figure 1. Targeted Disruption of the Mouse *Ikbns* Gene

(A) Maps of the IκBNS wild-type genome, targeting vector, and predicted targeted gene. Open and closed boxes denote the noncoding and coding exons, respectively. Restriction enzymes: S, ScaI.

(B) Southern blot analysis of offspring from the heterozygote intercrosses. Genomic DNA was extracted from mouse tails, digested with ScaI, electrophoresed, and hybridized with the probe indicated in (A). The approximate size of the wild-type band is 4.9 kb, and the mutated band is 3.6 kb.

(C) Peritoneal macrophages were cultured with or without 100 ng/ml LPS for 1 hr (L and M, respectively), and total RNA was extracted, electrophoresed, transferred to nylon membrane, and hybridized with the mouse IκBNS full-length cDNA probe. The same membrane was rehybridized with a GAPDH probe.

Results

Targeted Disruption of the IκBNS Gene

To study the functional role of IκBNS in TLR-dependent responses, a null mutation in the *Ikbns* allele was introduced through homologous recombination in embryonic stem (ES) cells (Figures 1A and 1B). IκBNS$^{-/-}$ mice were born alive and grew healthy until 20 weeks of age. We performed Northern blot analysis to confirm that the mutation causes inactivation of the *Ikbns* gene. LPS robustly induced IκBNS mRNA in wild-type macrophages, but not in IκBNS$^{-/-}$ macrophages (Figure 1C).

A previous report indicated that IκBNS is involved in negative selection of thymocytes (Fiorini et al., 2002). Therefore, we first analyzed lymphocyte composition in lymphoid organs such as thymus and spleen by flow cytometry (Figures S1A and S1B). Total cell number and CD4/CD8 or CD3/B220 populations in thymus and spleen were not altered in IκBNS$^{-/-}$ mice. Splenic T cells from IκBNS$^{-/-}$ mice showed similar levels of proliferative responses to IL-2 and IL-7 as did wild-type T cells. Moreover, IκBNS$^{-/-}$ T cells proliferated to almost equal degrees in response to anti-CD3 antibody compared to wild-type T cells (Figure S1C). These results indicate that T cell development and functions were generally unaffected in IκBNS$^{-/-}$ mice.

Increased IL-6 and IL-12p40 Production in IκBNS-Deficient Cells

Since IκBNS expression was induced within 1 hr of LPS stimulation in macrophages (Figure 1B), we stimulated peritoneal macrophages with various concentrations of LPS and analyzed for production of TNF-α and IL-6 (Figure 2A). In macrophages from IκBNS$^{-/-}$ mice, LPS-induced TNF-α production was comparable to wild-type cells, but IL-6 production was significantly increased. We then analyzed whether IκBNS$^{-/-}$ macrophages produce increased amounts of IL-6 in response to other TLR ligands, since IκBNS mRNA was induced by several TLR ligands as well as the TLR4 ligand LPS in a MyD88-dependent manner (Figure S2A). Peritoneal macrophages were stimulated with mycoplasmal lipopeptides (TLR6 ligand), Pam_3CSK_4 (TLR1 ligand), peptidoglycan (TLR2 ligand), and imiquimod (TLR7 ligand), and analyzed for production of TNF-α and IL-6 (Figure 2B). In response to these TLR ligands, the production of IL-6, but not TNF-α, was increased in IκBNS$^{-/-}$ mice. We next analyzed the response of bone marrow-derived dendritic cells (DCs). DCs from IκBNS$^{-/-}$ mice produced similar amounts of TNF-α and increased amounts of IL-6 in response to LPS compared to wild-type DCs (Figure 2C). In addition, DCs showed LPS-induced production of IL-12p40 and IL-12p70, and production of these

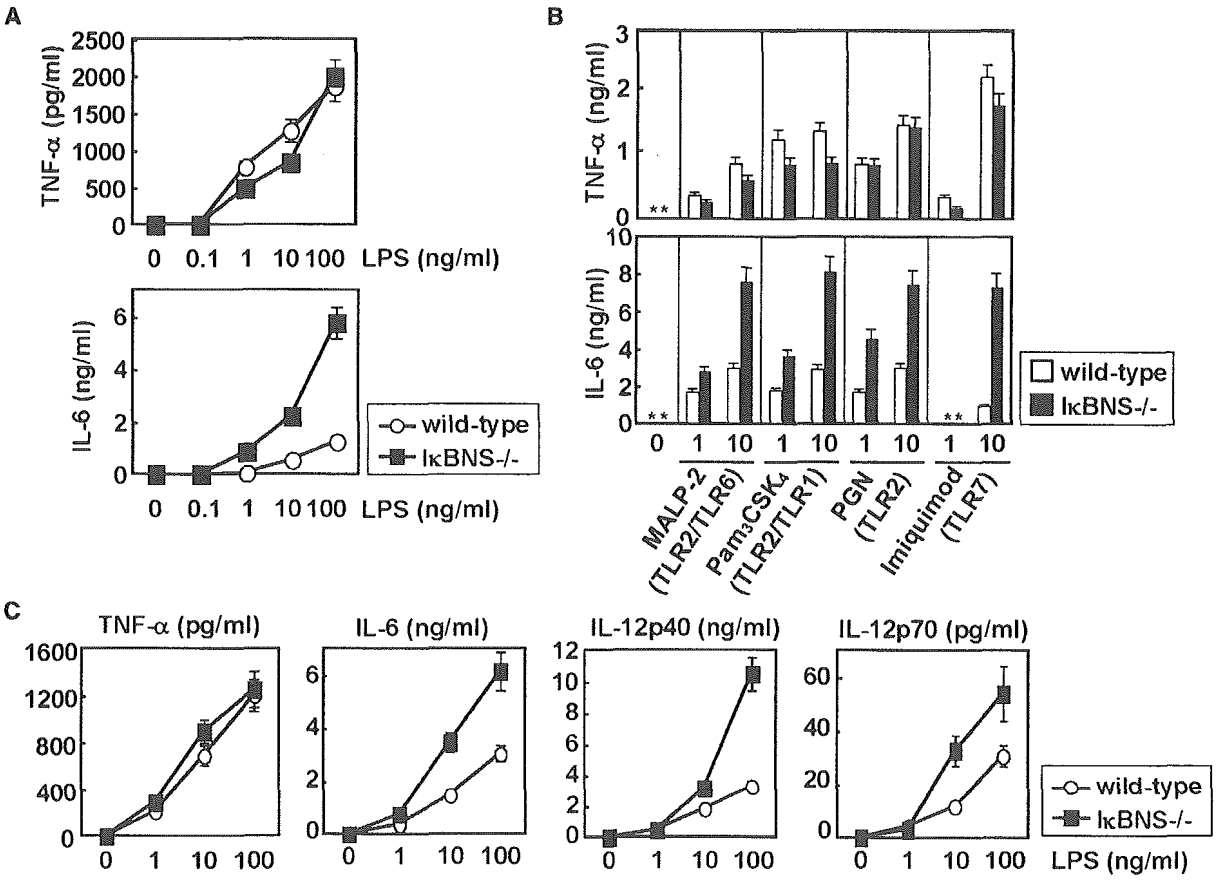

Figure 2. Increased Production of IL-6 and IL-12p40 in IκBNS$^{-/-}$ Macrophages and Dendritic Cells

(A) Peritoneal macrophages were stimulated with the indicated concentration of LPS for 24 hr. Concentrations of TNF-α and IL-6 in the culture supernatants were analyzed by ELISA. Data are mean ± SD of triplicate cultures in a single experiment, representative of three independent experiments.

(B) Peritoneal macrophages were cultured with 1 or 10 ng/ml of TLR6 ligand (MALP-2), 1 or 10 ng/ml TLR1 ligand (Pam_3CSK_4), 1 or 10 μg/ml TLR2 ligand (peptidoglycan; PGN), or 1 or 10 μg/ml TLR7 ligand (imiquimod) for 24 hr. Concentrations of TNF-α and IL-6 in the culture supernatants were analyzed by ELISA. *; not detected.

(C) Bone marrow-derived DCs were stimulated with the indicated concentration of LPS for 24 hr. Concentrations of TNF-α, IL-6, IL-12p40, and IL-12p70 in the culture supernatants were analyzed by ELISA. Data are mean ± SD of triplicate cultures in a single experiment, representative of three independent experiments.

cytokines was significantly increased in IκBNS$^{-/-}$ DCs. Bone marrow-derived DCs and splenic B cells were analyzed for LPS-induced surface expression of CD86 or MHC class II (Figure S2B). LPS-induced augmentation of surface expression of these molecules was not altered in IκBNS$^{-/-}$ mice. Thus, macrophages and DCs from IκBNS$^{-/-}$ mice showed selective increases in TLR-dependent production of IL-6 and IL-12p40.

Enhanced Induction of a Subset of TLR-Dependent Genes in IκBNS-Deficient Macrophages

We further analyzed LPS-induced mRNA expression of TLR-dependent genes in IκBNS$^{-/-}$ macrophages. Peritoneal macrophages were stimulated with LPS for 1, 3, or 5 hr, and total RNA was extracted. Then, mRNA expression of TNF-α and IL-6 was first analyzed by quantitative real-time RT-PCR (Figures 3A and 3B). LPS-induced TNF-α mRNA expression in IκBNS$^{-/-}$ macrophages was similar to wild-type cells. In the case of IL-6 mRNA, expression levels were comparable between wild-type and IκBNS$^{-/-}$ macrophages until 3 hr of LPS stimulation. After 3 hr, IL-6 mRNA levels decreased in wild-type cells. However, IκBNS$^{-/-}$ cells displayed further enhanced expression of IL-6 mRNA. TNF-α mRNA was robustly induced within 1 hr of LPS stimulation, and its expression promptly ceased in wild-type cells. In contrast, IL-6 mRNA expression was induced late compared to TNF-α. Because LPS-induced IκBNS mRNA expression showed similar patterns as TNF-α mRNA, we hypothesized that LPS-inducible IκBNS blocks mRNA expression of genes that are induced late (Figure 3C). Accordingly, we analyzed mRNA expression of other genes that are induced early (*Il-1β*, *Il-23p19*, or *Ikbz*) or late (*Il-12p40*, *Il-18*, or *Csf3*) in response to LPS. LPS-induced mRNA expression of *Il-1β* (IL-1β), *Il-23p19* (IL-23p19), and *Ikbz* (IκBζ) was similarly observed between wild-type and IκBNS$^{-/-}$ macrophages (Figure 3A). LPS-induced expression of *Il-12p40* (IL-12p40), *Il-18* (IL-18) and *Csf3* (G-CSF) was observed at normal levels in IκBNS$^{-/-}$ macrophages at the early phase of LPS stimulation (within 3 hr of LPS stimulation) (Figure 3B). However, at the late phase of LPS stimulation (after 3 hr of LPS stimulation), mRNA expression of these genes was significantly enhanced in

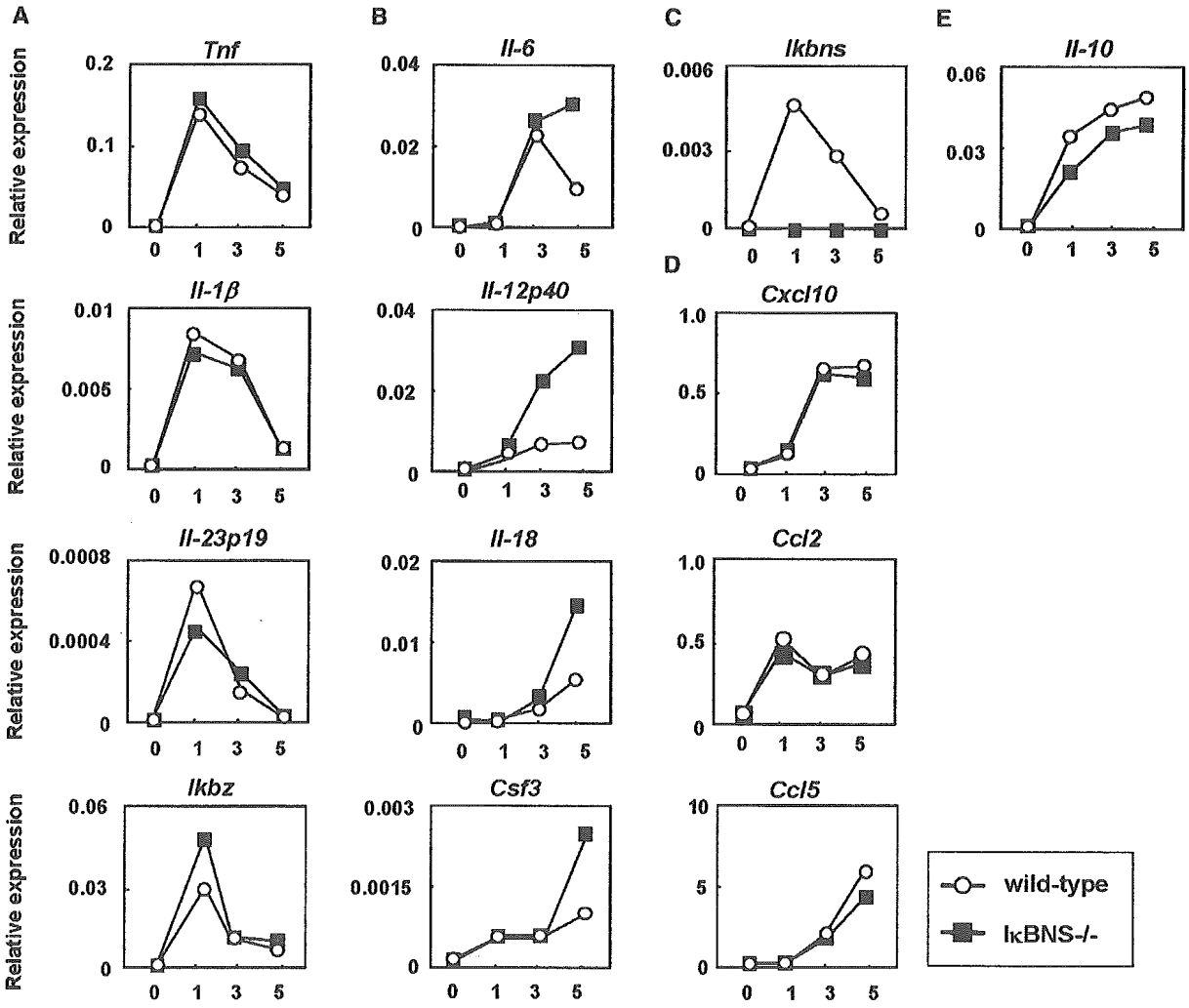

Figure 3. LPS-Induced Expression of Several TLR-Dependent Genes in IκBNS$^{-/-}$ Macrophages

Peritoneal macrophages from wild-type and IκBNS$^{-/-}$ mice were stimulated with 100 ng/ml LPS for the indicated periods. Total RNA was extracted, and then subjected to quantitative real-time RT-PCR analysis using primers specific for *Tnf*, *Il-1β*, *Il-23p19*, *Ikbz* (A), *Il-6*, *Il-12p40*, *Il-18*, *Csf3* (B), *Ikbns* (C), *Cxcl10*, *Ccl2*, *Ccl5* (D), and *Il-10* (E). The fold difference of each sample relative to EF-1α levels is shown. Representative of three independent experiments.

IκBNS$^{-/-}$ cells. We also analyzed LPS-induced expression of *Cxcl10* (IP-10), *Ccl2* (MCP-1), and *Ccl5* (RANTES), which are induced by the TRIF-dependent activation of IRF-3 (Figure 3D). LPS-induced expression of these genes was not altered in IκBNS$^{-/-}$ macrophages. An anti-inflammatory cytokine IL-10 is induced by TLR stimulation and thereby inhibits TLR-dependent gene induction (Moore et al., 2001). Therefore, we next addressed LPS-induced IL-10 mRNA expression (Figure 3E). LPS-induced IL-10 mRNA expression was comparable between wild-type and IκBNS$^{-/-}$ macrophages. In addition, LPS-induced production of IL-10 protein was not compromised in IκBNS$^{-/-}$ DCs (Figure S2C). These findings indicate that the enhanced LPS-induced expression of a subset of TLR-dependent genes was not due to the impaired IL-10 production in IκBNS$^{-/-}$ mice.

Prolonged NF-κB Activity in IκBNS-Deficient Cells

Gene expression of *Cxcl10* (IP-10), *Ccl2* (MCP-1), and *Ccl5* (RANTES) was mainly regulated by the transcription factor IRF-3 in the TRIF-dependent pathway, whereas TNF-α, IL-6, and IL-12p40 gene expression was mainly regulated by the MyD88-dependent activation of NF-κB (Akira and Takeda, 2004; Yamamoto et al., 2003). In addition, previous in vitro studies indicated that overexpression of IκBNS leads to compromised NF-κB activity through selective association of IκBNS with p50 subunit of NF-κB (Fiorini et al., 2002; Hirotani et al., 2005). Therefore, we next analyzed LPS-induced activation of NF-κB. LPS-induced degradation of IκBα was not compromised in IκBNS$^{-/-}$ macrophages (Figure S3A). Next, peritoneal macrophages or bone marrow-derived macrophages were stimulated with LPS and DNA binding activity was analyzed by EMSA (Figure 4A; Figure S3B). LPS stimulation resulted in enhanced DNA binding activity of NF-κB in both wild-type and IκBNS$^{-/-}$ macrophages to similar extents within 1 hr. After 1 hr of LPS stimulation, NF-κB activity decreased in wild-type cells. However, NF-κB activity sustained and even at 3 hr of LPS stimulation significant DNA binding activity was still observed in

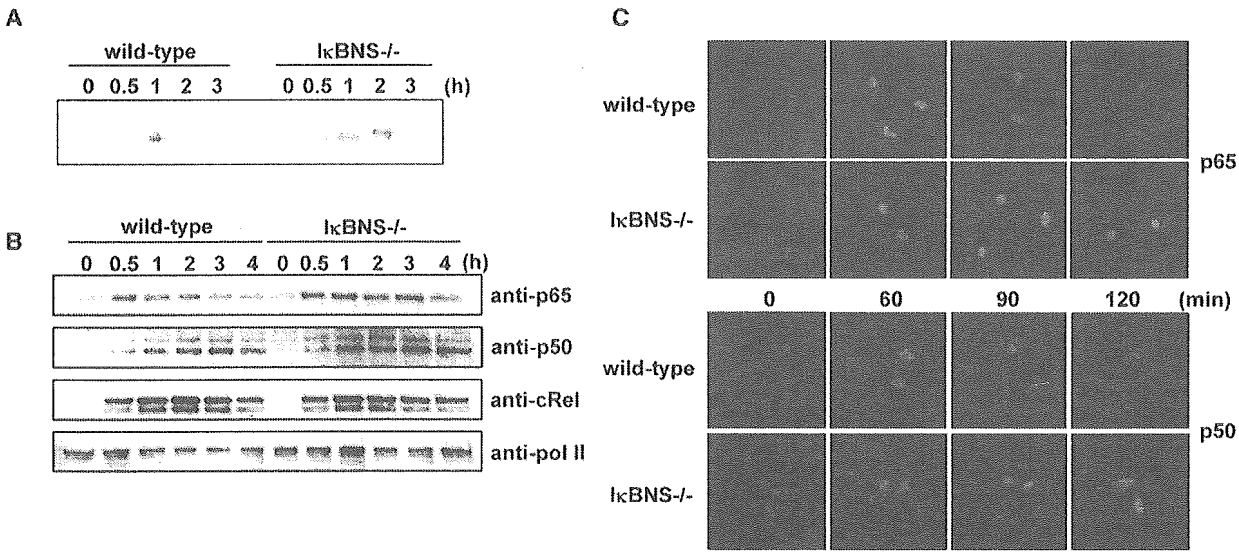

Figure 4. Persistent LPS-Induced Activation of NF-κB in IκBNS$^{-/-}$ Macrophages

(A) Peritoneal macrophages from wild-type and IκBNS$^{-/-}$ mice were stimulated with 100 ng/ml LPS. At the indicated time points, nuclear extracts were prepared, and NF-κB activation was analyzed by EMSA using a NF-κB specific probe.

(B) Peritoneal macrophages were stimulated with LPS. At the indicated time points, nuclear fractions were isolated and subjected to Western blotting using anti-p65 Ab, anti-p50 Ab, anti-cRel Ab, or anti-polII Ab.

(C) Macrophages were stimulated with LPS for the indicated periods. Then, cells were stained with anti-p65 Ab or anti-p50 Ab (red) as well as DAPI (blue), and analyzed by confocal microscopy. Merged images are shown.

IκBNS$^{-/-}$ cells. We next analyzed nuclear localization of NF-κB subunits. Peritoneal macrophages were stimulated with LPS for the indicated periods, and nuclear fractions were analyzed for expression of p65, p50, and c-Rel by immunoblotting (Figure 4B). In wild-type macrophages, nuclear translocation of p65 was observed within 30 min of LPS stimulation, and nuclear localized p65 gradually decreased thereafter. In contrast, nuclear localized p65 was still significantly observed even at 3 hr of LPS stimulation in IκBNS$^{-/-}$ cells. In addition, sustained nuclear localization of p50, but not c-Rel, was observed in IκBNS$^{-/-}$ macrophages (Figure 4B). Nuclear localization of NF-κB subunits was also analyzed by immunofluorescent staining of macrophages (Figure 4C). Without stimulation, p65 and p50 were localized in the cytoplasm, but not in the nucleus, in both wild-type and IκBNS$^{-/-}$ macrophages. LPS stimulation resulted in nuclear staining of both p65 and p50 at 1 hr. Nuclear staining of p65 and p50 gradually decreased after 1 hr of LPS stimulation and was only faintly observed at 2 hr of stimulation in wild-type cells. However, nuclear localization of p65 and p50 was still evident at 2 hr of LPS stimulation in IκBNS$^{-/-}$ cells. These findings indicate that LPS-induced NF-κB activity was prolonged in IκBNS$^{-/-}$ macrophages. NF-κB activity is terminated by degradation of promoter-bound p65 (Natoli et al., 2005; Saccani et al., 2004). We used RAW264.7 macrophage cell line and performed pulse-chase experiments with ^{35}S-labeled amino acids to analyze p65 turnover (Figure S3C). In these cells, labeled p65 was accumulated into the nucleus until 2 hr of LPS stimulation, and then p65 was degraded. In RAW cells constitutively expressing IκBNS, nuclear accumulation of labeled p65 was similarly observed until 1 hr of LPS stimulation. However, the p65 turnover was observed more rapidly and labeled p65 disappeared at 2 hr after LPS stimulation (Figure S3C). These findings indicate that IκBNS mediates the degradation of p65. The MyD88-dependent pathway mediates activation of MAP kinase cascades as well as NF-κB activation. Therefore, LPS-induced phosphorylation of p38, ERK1, ERK2, and JNK was analyzed by Western blotting (Figure S3D). LPS-induced activation of these MAP kinases was not compromised in IκBNS$^{-/-}$ macrophages.

Regulation of p65 Activity at the IL-6 Promoter by IκBNS

We next addressed how IκBNS selectively downregulates induction of genes that are induced late. We utilized the IL-6 and TNF-α promoters, which are representatives of genes activated late and early, respectively. Wild-type macrophages were stimulated with LPS and analyzed for recruitment of endogenous IκBNS to the promoters by chromatin immunoprecipitation (ChIP) assay (Figure 5A). Consistent with previous findings using IκBNS overexpressing macrophage cell lines (Hirotani et al., 2005), endogenous IκBNS was recruited to the IL-6 promoter, but not the TNF-α promoter, in LPS-stimulated macrophages. We next addressed LPS-induced recruitment of p65 to the promoters in wild-type and IκBNS$^{-/-}$ macrophages (Figure 5B). Recruitment of p65 to the TNF-α promoter peaked at 1 hr of LPS stimulation and gradually decreased thereafter in a similar manner in both wild-type and IκBNS$^{-/-}$ cells. Recruitment of p65 to the IL-6 promoter was observed to similar extents until 3 hr of LPS stimulation in wild-type and IκBNS$^{-/-}$ macrophages. After that, it decreased in wild-type macrophages. In contrast, p65 recruitment was still evident, rather enhanced, even after 5 hr of LPS stimulation in IκBNS$^{-/-}$ macrophages. Thus, p65 activity at

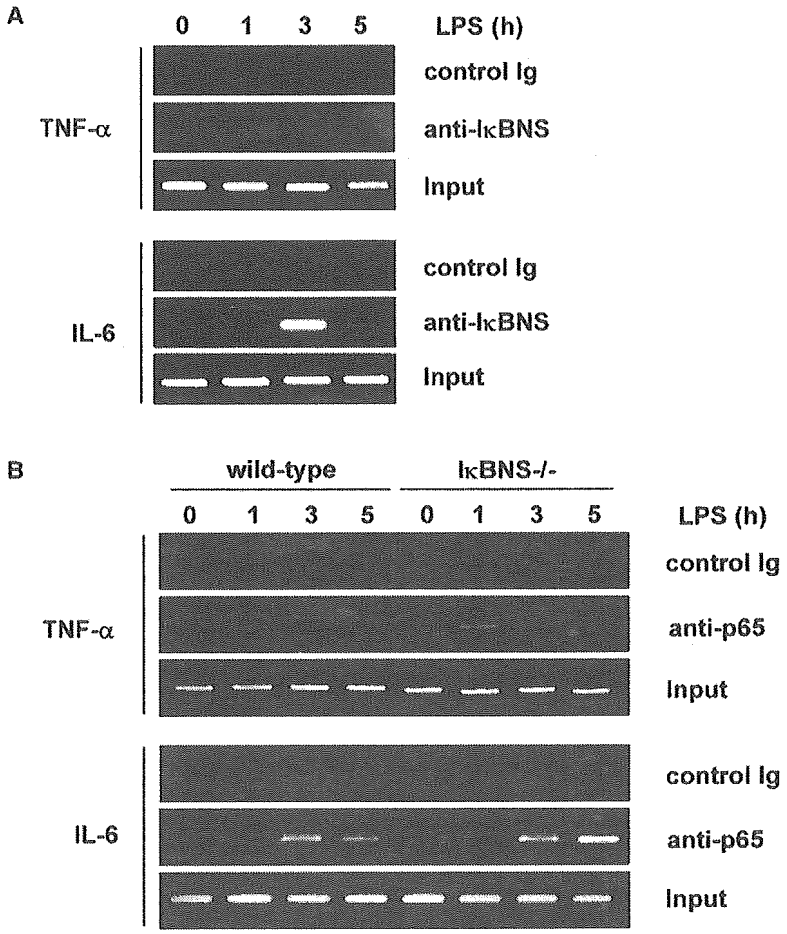

Figure 5. IκBNS Regulation of p65 Activity at the IL-6 Promoter

(A) Wild-type bone marrow-derived macrophages were stimulated with 100 ng/ml of LPS for the indicated periods, and chromatin immunoprecipitation (ChIP) assay was performed with anti-IκBNS Ab or control Ig. The immunoprecipitated TNF-α promoter (upper panel) or IL-6 promoter (lower panel) was analyzed by PCR with promoter-specific primers. PCR amplification of the total input DNA in each sample is shown (Input). Representative of three independent experiments. The same result was obtained when peritoneal macrophages were used.

(B) Macrophages from wild-type or IκBNS$^{-/-}$ mice were stimulated with LPS for the indicated periods. Then, ChIP assay was performed with anti-p65 Ab or control Ig. The immunoprecipitated TNF-α promoter (upper panel) or IL-6 promoter (lower panel) was analyzed by PCR with promoter-specific primers. Representative of three independent experiments.

the IL-6 promoter, but not at the TNF-α promoter, was prolonged in LPS-stimulated IκBNS$^{-/-}$ macrophages. Taken together, these findings indicate that TLR-inducible IκBNS is responsible for termination of NF-κB activity through its recruitment to specific promoters.

High Sensitivity to LPS-Induced Endotoxin Shock in IκBNS-Deficient Mice

To study the in vivo role of IκBNS, we examined LPS-induced endotoxin shock. Intraperitoneal injection of LPS resulted in marked increases in serum concentrations of TNF-α, IL-6, and IL-12p40 (Figure 6A). TNF-α level was comparable between wild-type and IκBNS$^{-/-}$ mice, which rapidly peaked at around 1.5 hr of LPS administration. In the case of IL-6 and IL-12p40 levels, concentrations of both cytokines were almost equally elevated within 3 hr of LPS injection. After 3 hr, levels of both cytokines gradually decreased in wild-type mice. However, concentrations of IL-6 and IL-12p40 sustained, rather enhanced, in IκBNS$^{-/-}$ mice after 3 hr. Thus, persistently high concentrations of LPS-induced serum IL-6 and IL-12p40 were observed in IκBNS$^{-/-}$ mice. Furthermore, high sensitivity to LPS-induced lethality was observed in IκBNS$^{-/-}$ mice (Figure 6B). All IκBNS$^{-/-}$ mice died within 4 days of LPS challenge at a dose of which almost all wild-type mice survived over 4 days. These findings indicate that IκBNS$^{-/-}$ mice are highly sensitive to LPS-induced endotoxin shock.

High Susceptibility to DSS-Induced Colitis in IκBNS$^{-/-}$ Mice

In a previous report, IκBNS was shown to be constitutively expressed in macrophages residing in the colonic lamina propria, which explains one of the mechanisms for hyporesponsiveness to TLR stimulation in these cells (Hirotani et al., 2005). Therefore, we next stimulated CD11b^{+} cells isolated from the colonic lamina propria with LPS and analyzed for production of TNF-α and IL-6 (Figure S4). In CD11b^{+} cells from wild-type mice, LPS-induced production of these cytokines was not significantly observed. In cells from IκBNS$^{-/-}$ mice, IL-6 production was increased even in the absence of stimulation, and LPS stimulation led to markedly enhanced production of IL-6, but not TNF-α. In the next experiment, in order to expose these cells to microflora and cause intestinal inflammation, mice were orally administered with dextran sodium sulfate (DSS), which is toxic to colonic epithelial cells and therefore disrupts the epithelial cell barrier (Kitajima et al., 1999). IκBNS$^{-/-}$ mice showed more severe weight loss compared with wild-type mice (Figure 7A). Histological analyses of the colon indicated that the inflammatory lesions were more severe and more extensive in IκBNS$^{-/-}$ mice (Figures 7B and 7C). Thus, IκBNS$^{-/-}$ mice are highly susceptible to intestinal inflammation. Th1-oriented CD4^{+} T cell response was shown to be associated with DSS colitis (Strober et al., 2002). Therefore, we analyzed IFN-γ

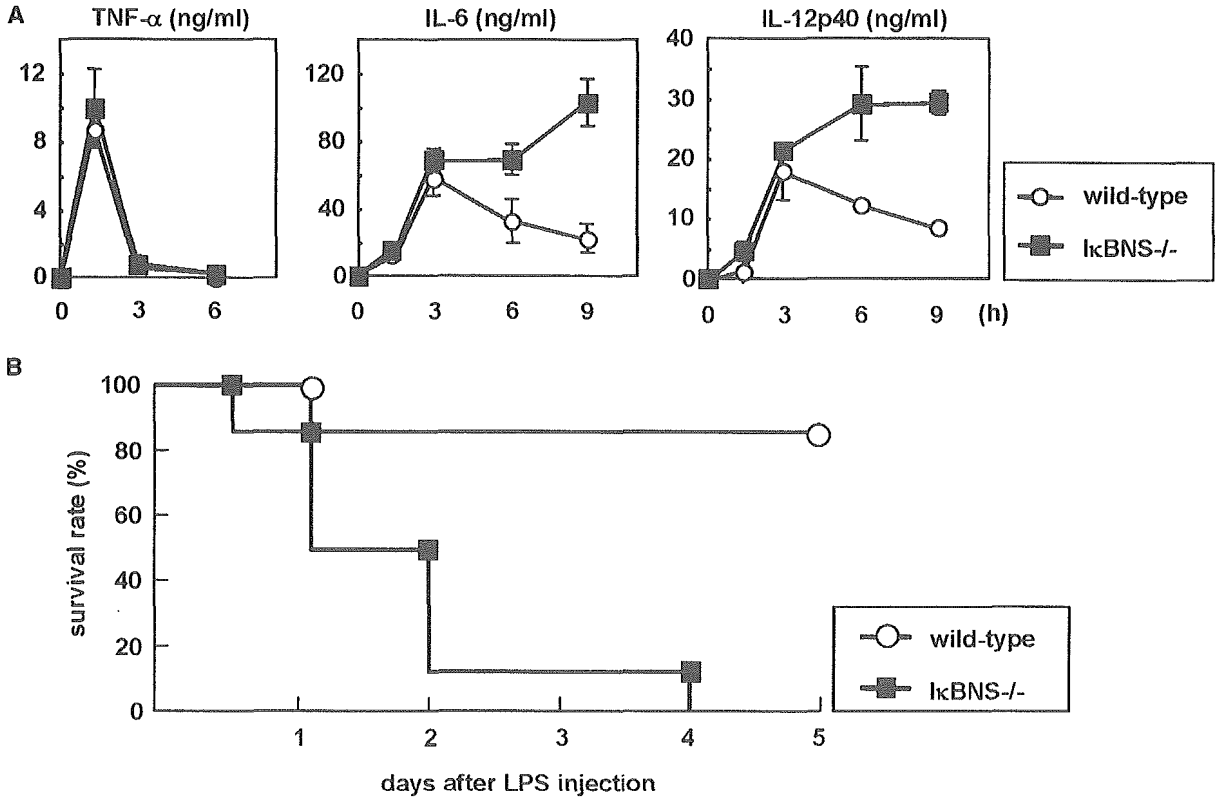

Figure 6. High Susceptibility to LPS-Induced Endotoxin Shock in IκBNS$^{-/-}$ Mice

Age-matched wild-type (n = 6) and IκBNS−/− (n = 6) mice were intraperitoneally injected with LPS (1 mg). (A) Sera were taken at 1.5, 3, 6, and 9 hr after LPS injection. Serum concentrations of TNF-α, IL-6, and IL-12p40 were determined by ELISA. Results are shown as mean ± SD of serum samples from six mice. (B) Survival was monitored for 5 days.

production from splenic CD4$^+$ T cells of wild-type and IκBNS$^{-/-}$ mice before and after DSS administration (Figure 7D). DSS administration led to a mild increase in IFN-γ production in wild-type mice. In nontreated IκBNS$^{-/-}$ mice, IFN-γ production was slightly increased compared with nontreated wild-type mice. In DSS-fed IκBNS$^{-/-}$ mice, a significant increase in IFN-γ production was observed compared to DSS-fed wild-type mice. These results indicate that IκBNS$^{-/-}$ mice are susceptible to intestinal inflammation caused by exposure to microflora.

Discussion

In the present study, we characterized the physiological function of IκBNS. Induced by TLR stimulation, IκBNS is involved in termination of NF-κB activity and thereby inhibits a subset of TLR-dependent genes that are induced late through MyD88-dependent NF-κB activation. Accordingly, IκBNS$^{-/-}$ mice show sustained production of IL-6 and IL-12p40, resulting in high susceptibility to LPS-induced endotoxin shock. Furthermore, IκBNS$^{-/-}$ mice are susceptible to intestinal inflammation accompanied by enhanced Th1 responses.

IκBNS was originally identified as a molecule that mediates negative selection of thymocytes (Fiorini et al., 2002). However, IκBNS$^{-/-}$ mice did not show any defect in T cell development. Requirement of IκBNS in negative selection of thymocytes should be analyzed precisely using peptide-specific TCR transgenic mice, such as mice bearing the H-Y TCR, in the future (Kisielow et al., 1988).

Recent studies have established that TLR-dependent gene induction is regulated mainly by NF-κB and IRF families of transcription factors (Akira and Takeda, 2004; Honda et al., 2005; Takaoka et al., 2005). In TLR4 signaling, the TRIF-dependent pathway is responsible for induction of IFN-β and IFN-inducible genes through activation of IRF-3, whereas the MyD88-dependent pathway mediates induction of several NF-κB dependent genes (Beutler, 2004). A study with mice lacking IκBζ, another member of nuclear IκB proteins, has demonstrated that the MyD88-dependent genes are divided into at least two types; one is induced early and independent of IκBζ, and another is induced late and dependent on IκBζ (Yamamoto et al., 2004). The IκBζ-regulated genes include IL-6, IL-12p40, IL-18, and G-CSF, which are all upregulated in LPS-stimulated IκBNS$^{-/-}$ macrophages. Thus, IκBNS seems to possess a function quite opposite to IκBζ. IκBNS is most structurally related to IκBζ (Fiorini et al., 2002; Hirotani et al., 2005). But, IκBζ has an additional N-terminal structure, which seemingly mediates the induction of target genes (Motoyama et al., 2005). Thus, nuclear IκB proteins IκBζ and IκBNS positively and negatively regulate a subset of TLR-induced NF-κB-dependent genes, respectively.

Recently, negative regulation of TLR-dependent gene induction was extensively analyzed (Liew et al., 2005).

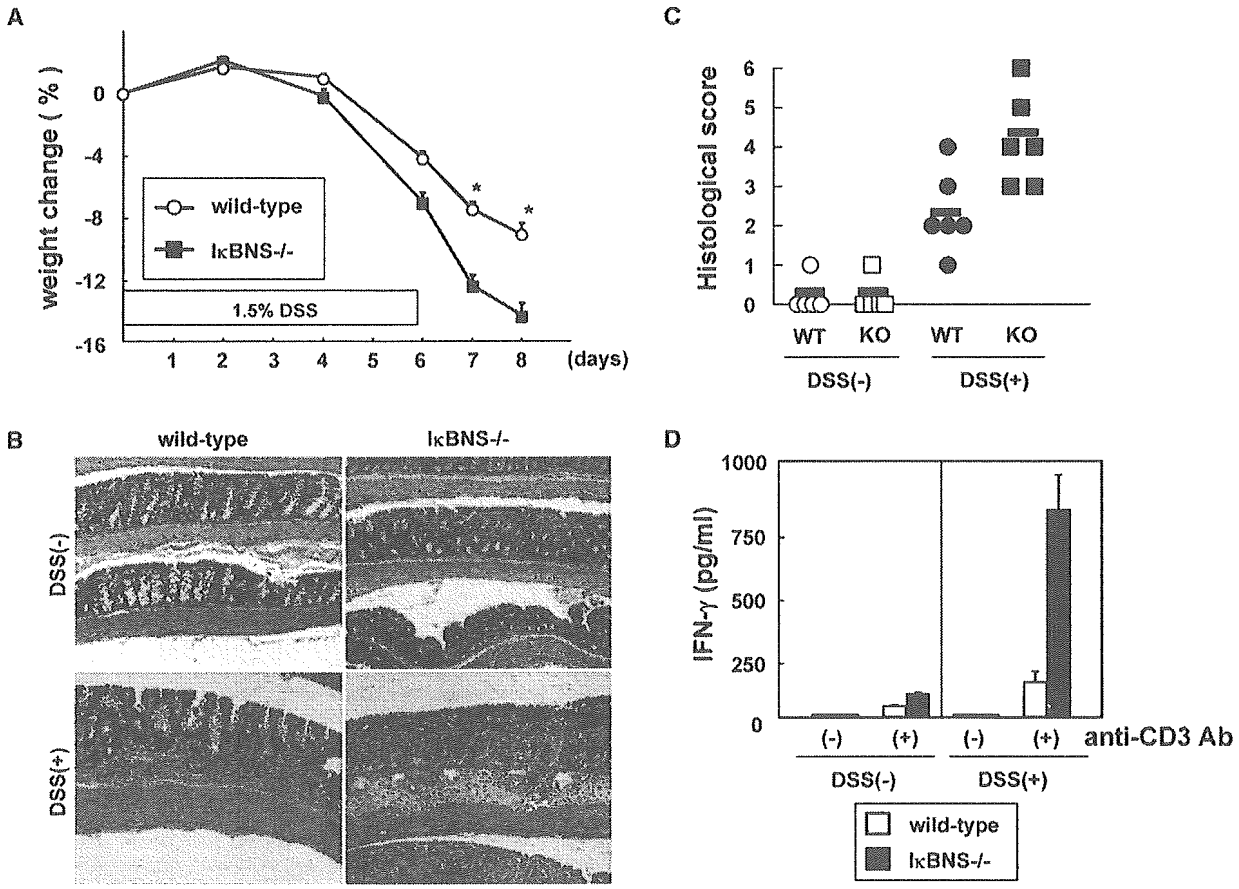

Figure 7. High Susceptibility to DSS Colitis in IκBNS$^{-/-}$ Mice

(A) Wild-type (n = 15) and IκBNS$^{-/-}$ mice (n = 15) were given 1.5% DSS in drinking water for 6 days and weighed everyday. Data are mean ± SD. *, $p < 0.05$.

(B) Histologic examination of the colons of wild-type and IκBNS$^{-/-}$ mice before or 9 days after initiation of DSS administration. H&E staining is shown. Representative of six mice examined. Magnification, 20×.

(C) The colitis scores shown for individual wild-type (circle) and IκBNS$^{-/-}$ mice (square) before (open) and after (closed) DSS treatment were total scores for individual sections as described in the Experimental Procedures section. Mean score for each group is also shown (black bar).

(D) CD4$^+$ T cells were purified from spleen of wild-type or IκBNS$^{-/-}$ mice either treated or nontreated with DSS. Then, CD4$^+$ T cells were cultured in the presence or absence of plate bound anti-CD3 Ab for 24 hr. Concentration of IFN-γ in the culture supernatants was measured by ELISA.

So far, characterized negative regulators are mainly involved in blockade of TLR signaling pathways in the cytoplasm or on the cell membrane. Accordingly, these negative regulators globally inhibit TLR-dependent gene induction. The nuclear IκB protein IκBNS is unique in that this molecule negatively regulates induction of a set of TLR-dependent genes by directly affecting NF-κB activity in the nucleus. Thus, TLR-dependent innate immune responses are regulated through a variety of mechanisms.

IκBNS-mediated inhibition of a set of TLR-dependent genes is probably explained by recruitment of IκBNS to the specific promoters. IκBNS was recruited to the IL-6 promoter, but not to the TNF-α promoter. In addition, LPS-induced recruitment of p65 to the TNF-α promoter was observed within 1 hr, whereas p65 recruitment to the IL-6 promoter was observed late, indicating that NF-κB activity was differentially regulated at both promoters. NF-κB activity at the TNF-α promoter is regulated in an IκBNS-independent manner, whereas the activity at the IL-6 promoter was IκBNS-dependent. Indeed, p65 recruitment to the TNF-α promoter was observed similarly in wild-type and IκBNS$^{-/-}$ macrophages, but the recruitment to the IL-6 promoter was sustained in IκBNS$^{-/-}$ cells. Previous reports indicate that IκBNS selectively associates with p50 subunit of NF-κB and affects NF-κB DNA binding activity (Fiorini et al., 2002; Hirotani et al., 2005). Consistent with these observations, IκBNS$^{-/-}$ macrophages showed prolonged LPS-induced NF-κB DNA binding activity and nuclear localization of p65. Taken together, these findings indicate that IκBNS, which is rapidly induced by TLR stimulation, might be recruited to gene promoters through association with p50, and contribute to termination of NF-κB activity. Termination of NF-κB activity has been shown to be induced by IKKα-mediated degradation of promoter-bound p65 (Lawrence et al., 2005). However, consistent with a recent report, we were not able to detect LPS-induced degradation of p65 in peritoneal macrophages and bone marrow-derived macrophages (Li et al., 2005). However, we could detect LPS-induced p65 degradation in the RAW264.7 macrophage cell line. In these cells, when constitutively expressed IκBNS, LPS-induced p65 turnover was

accelerated, indicating that IκBNS is involved in the degradation of promoter-bound p65. In the case of the TNF-α promoter, it is possible that NF-κB activity is already terminated when IκBNS expression is induced, and therefore IκBNS is no longer recruited to the TNF-α promoter. Alternatively, an unidentified mechanism that regulates selective recruitment of IκBNS to gene promoters might exist. The mechanisms by which IκBNS is recruited to the specific promoters through association with p50 remain unclear and would be a subject of further investigation.

Analyses of IκBNS$^{-/-}$ mice further highlighted the in vivo functions of IκBNS in limiting systemic and intestinal inflammation. IκBNS$^{-/-}$ mice succumbed to systemic LPS-induced endotoxin shock possibly due to sustained production of several TLR-dependent gene products such as IL-6 and IL-12p40. Furthermore, IκBNS$^{-/-}$ mice are more susceptible to intestinal inflammation induced by disruption of the epithelial barrier. Abnormal activation of innate immune cells caused by deficiency of IL-10 or Stat3 leads to spontaneous development of colonic inflammation (Kobayashi et al., 2003; Kuhn et al., 1993; Takeda et al., 1999). IκBNS$^{-/-}$ mice did not develop chronic colitis spontaneously until 20 week-old of age (our unpublished data). In Stat3 mutant mice, TLR-dependent production of proinflammatory cytokines increased over 10-fold compared to wild-type cells, which might contribute to the spontaneous intestinal inflammation (Takeda et al., 1999). In IκBNS$^{-/-}$ mice, increase in TLR-dependent production of proinflammatory cytokines such as IL-6 and IL-12p40 was mild compared to Stat3 mutant mice. In this case, the colonic epithelial barrier might contribute to prevention of excessive inflammatory responses in IκBNS$^{-/-}$ mice. However, when the barrier function of epithelial cells was disrupted by administration of DSS, IκBNS$^{-/-}$ mice suffered from severe intestinal inflammation accompanied by enhanced Th1 responses. IκBNS was shown to be expressed in CD11b^{+} cells residing in the colonic lamina propria (Hirotani et al., 2005). Therefore, in the absence of IκBNS, exposure of innate immune cells to intestinal microflora might result in increased or sustained production of proinflammatory cytokines such as IL-12p40, which induces exaggerated intestinal inflammation and Th1 cell development. Thus, IκBNS is responsible for the prevention of uncontrolled inflammatory responses in vivo.

In this study, we have shown that IκBNS is a selective inhibitor of TLR-dependent genes possibly through termination of NF-κB activity. Furthermore, IκBNS was responsible for prevention of inflammation through inhibition of persistent proinflammatory cytokine production. Future study that discloses the precise molecular mechanisms by which the nuclear IκB protein selectively inhibits TLR-dependent genes will provide basis for the development of new therapeutic strategies to a variety of inflammatory diseases.

Experimental Procedures

Generation of IκBNS-Deficient Mice

The *Ikbns* gene consists of eight exons (Figure 1A). The targeting vector was designed to replace a 1.8 kb fragment containing exons 5–8 of the *Ikbns* gene with a neomycin-resistance gene (*neo*). A short arm and a long arm of the homology region from the E14.1 ES genome were amplified by PCR. A herpes simplex virus thymidine kinase gene (HSV-TK) was inserted into the 3′ end of the vector. After the targeting vector was electroporated into ES cells, G418 and gancyclovir doubly resistant clones were selected and screened for homologous recombination by PCR and verified by Southern blot analysis using the probe indicated in Figure 1A. Two independently identified targeted ES clones were microinjected into C57BL/6 blastocysts. Chimeric mice were mated with C57BL/6 female mice, and heterozygous F1 progenies were intercrossed to obtain IκBNS$^{-/-}$ mice. Mice from these independent ES clones displayed identical phenotypes. All animal experiments were conducted according to guidelines of Animal Care and Use Committee at Kyushu University.

Reagents

LPS (*E. coli* 055:B5) was purchased from Sigma. Peptidoglycan was from Fluca. Pam_3CSK_4, MALP-2, and imiquimod were from Invivogen. Antibodies against p65 (C-20; sc-372), p50 (H-119; sc-7178 or NLS; sc-114), c-Rel (C; sc-71), and RNA polymerase II (H-224; sc-9001) were purchased from Santa Cruz. Rabbit anti-IκBNS Ab was generated against synthetic peptide (1-MEDSLDTRLY PEPSLSQVC-18) corresponding to N-terminal region of mouse IκBNS (MBL, Nagoya, Japan), and anti-IκBNS serum was affinity-purified using a column containing peptide-conjugated Sepharose 4B.

Preparation of Macrophages and Dendritic Cells

For isolation of peritoneal macrophages, mice were intraperitoneally injected with 2 ml of 4% thioglycollate medium (Sigma). Peritoneal exudate cells were isolated from the peritoneal cavity 3 days post injection. Cells were incubated for 2 hr and washed three times with HBSS. Remaining adherent cells were used as peritoneal macrophages for the experiments. To prepare bone marrow-derived macrophages, bone marrow cells were prepared from femora and tibia and passed through nylon mesh. Then cells were cultured in RPMI 1640 medium supplemented with 10% FCS, 100 μM 2-ME, and 10 ng/ml M-CSF (GenzymeTechne). After 6–8 days, the cells were used as macrophages for the experiments. Bone marrow-derived DCs were prepared by culturing bone marrow cells in RPMI 1640 medium supplemented with 10% FCS, 100 μM 2-ME, and 10 ng/ml GM-CSF (GenzymeTechne). After 6 days, the cells were used as DCs.

Measurement of Cytokine Production

Peritoneal macrophages or DCs were stimulated with various TLR ligands for 24 hr. Culture supernatants were collected and analyzed for TNF-α, IL-6, IL-12p40, IL-12p70, or IL-10 production with enzyme-linked immunosorbent assay (ELISA). Mice were intravenously injected with 1mg of LPS and bled at the indicated periods. Serum concentrations of TNF-α, IL-6, and IL-12p40 were determined by ELISA. ELISA kits were purchased from GenzymeTechne and R&D Systems. For measurement of IFN-γ, CD4^{+} T cells were purified from spleen cells using CD4 microbeads (Miltenyi Biotec) and stimulated by plate bound anti-CD3ε antibody (145-2C11, BD PharMingen) for 24 hr. Concentrations of IFN-γ in the supernatants were determined by ELISA (GenzymeTechne).

Quantitative Real-Time RT-PCR

Total RNA was isolated with TRIzol reagent (Invitrogen, Carlsbad, CA), and 2 μg of RNA was reverse transcribed using M-MLV reverse transcriptase (Promega, Madison, WI) and oligo (dT) primers (Toyobo, Osaka, Japan) after treatment with RQ1 DNase I (Promega). Quantitative real-time PCR was performed on an ABI 7700 (Applied Biosystems, Foster City, CA) using TaqMan Universal PCR Master Mix (Applied Biosystems). All data were normalized to the corresponding elongation factor-1α (EF-1α) expression, and the fold difference relative to the EF-1α level was shown. Amplification conditions were: 50°C (2 min), 95°C (10 min), 40 cycles of 95°C (15 s), and 60°C (60 s). Each experiment was performed independently at least three times, and the results of one representative experiment are shown. All primers were purchased from Assay on Demand (Applied Biosystems).

Electrophoretic Mobility Shift Assay

Macrophages were stimulated with 100 ng/ml LPS for the indicated periods. Then, nuclear proteins were extracted, and incubated with an end-labeled, double-stranded oligonucleotide containing an NF-κB binding site of the IL-6 promoter in 25 μl of binding buffer (10 mM HEPES-KOH, [pH 7.8], 50 mM KCl, 1 mM EDTA [pH 8.0], 5 mM $MgCl_2$ and 10% glycerol) for 20 min at room temperature and loaded on a native 5% polyacrylamide gel. The DNA-protein complexes were visualized by autoradiography.

Western Blotting

Cells were lysed with RIPA buffer (50 mM Tris-HCl [pH 7.5], 150 mM NaCl, 1% Triton X-100, 0.5% Na-deoxycholate) containing protease inhibitors (Complete Mini; Roche). The lysates were separated on SDS-PAGE and transferred to PVDF membrane. The membranes were incubated with anti-IκBα Ab, anti-ERK Ab, anti-p38 Ab, anti-JNK Ab (Santa Cruz Biotechnology), anti-phospho-p38 Ab, anti-phospho-ERK Ab, or anti-phospho-JNK Ab (Cell Signaling Technology). Bound Abs were detected with SuperSignal West Pico Chemiluminescent Substrate (Pierce).

Immunofluorescence Staining

Macrophages were stimulated with 100 ng/ml LPS for the indicated periods, washed with Tris-buffered saline (TBS), and fixed with 3.7% formaldehyde in TBS for 15 min at room temperature. After permeabilization with 0.2% Triton X-100, cells were washed with TBS and incubated with 10 ng/ml of a rabbit anti-p50 or anti-p65 Ab (Santa Cruz Biotechnology) in TBS containing 1% bovine serum albumin, followed by incubation with Alexa Fluor 594-conjugated goat anti-rabbit immunoglobulin G (IgG; Molecular Probes, Eugene, OR). To stain the nucleus, cells were cultured with 0.5 μg/ml 4, 6-diamidino-2-phenylindole (DAPI; Wako, Osaka, Japan). Stained cells were analyzed using an LSM510 model confocal microscope (Carl Zeiss, Oberkochem, Germany).

Chromatin Immunoprecipitation

Chromatin immunoprecipitation (ChIP) was performed essentially with a described protocol (Upstate Biotechnology, Lake Placid, NY). In brief, peritoneal macrophages from wild-type and $I\kappa BNS^{-/-}$ mice were stimulated with 100 ng/ml LPS for 1, 3, or 5 hr, and then fixed with formaldehyde for 10 min. The cells were lysed, sheared by sonication using Bioruptor (CosmoBio), and incubated overnight with specific antibody followed by incubation with protein A-agarose saturated with salmon sperm DNA (Upsate Biotechnology). Precipitated DNA was analyzed by quantitative PCR (35 cycles) using primers 5′- CCCCAGATTGCCACAGAATC -3′ and 5′- CCAGT GAGTGAAAGGGACAG -3′ for the TNF-α promoter and 5′- TGTGTG TCGTCTGTCATGCG-3′ and 5′- AGCTACAGACATCCCCAGTCTC -3′ for the IL-6 promoter.

Induction of DSS Colitis

Mice received 1.5% (wt/vol) DSS (40,000 kDa; ICN Biochemicals), ad libitum, in their drinking water for 6 days, then switched to regular drinking water. The amount of DSS water drank per animal was recorded and no differences in intake between strains were observed. Mice were weighed for the determination of percent weight change. This was calculated as: percentage weight change = (weight at day X-day 0/weight at day 0) × 100. Statistical significance was determined by paired Student's t test. Differences were considered to be statistically significant at $p < 0.05$.

Histological Analysis

Colon tissues were fixed in 4% paraformaldehyde, rolled up, and embedded in paraffin in a Swiss roll orientation such that the entire length of the intestinal tract could be identified on single sections. After sectioning, the tissues were dewaxed in ethanol, rehydrated, and stained hematoxylin and eosin to study histological changes after DSS-induced damage. Histological scoring was performed in a blinded fashion by a pathologist, with a combined score for inflammatory cell infiltration (score, 0–3) and tissue damage (score, 0–3) (Araki et al., 2005). The presence of occasional inflammatory cells in the lamina propria was assigned a value of 0; increased numbers of inflammatory cells in the lamina propria as 1; confluence of inflammatory cells, extending into the submucosa, as 2; and transmural extension of the infiltrate as 3. For tissue damage, no mucosal damage was scored as 0; discrete lymphoepithelial lesions were scored as 1; surface mucosal erosion or focal ulceration was scored as 2; and extensive mucosal damage and extension into deeper structures of the bowel wall were scored as 3. The combined histological score ranged from 0 (no changes) to 6 (extensive cell infiltration and tissue damage).

Supplemental Data

Supplemental Data include four figures and are available with this article online at http://www.immunity.com/cgi/content/full/24/1/41/DC1/.

Acknowledgments

We thank Y. Yamada, K. Takeda, M. Otsu, and N. Kinoshita for technical assistance; M. Yamamoto and S. Akira for providing us with reagents, P. Lee for critical reading of the manuscript, and M. Kurata for secretarial assistance. This work was supported by grants from the Special Coordination Funds of the Ministry of Education, Culture, Sports, Science and Technology; the Uehara Memorial Foundation; the Mitsubishi Foundation; the Takeda Science Foundation; the Tokyo Biochemical Research Foundation; the Kowa Life Science Foundation; the Osaka Foundation for Promotion of Clinical Immunology; and the Sankyo Foundation of Life Science.

Received: July 15, 2005
Revised: September 16, 2005
Accepted: November 16, 2005
Published: January 17, 2006

References

Akira, S., and Takeda, K. (2004). Toll-like receptor signalling. Nat. Rev. Immunol. *4*, 499–511.

Araki, A., Kanai, T., Ishikura, T., Makita, S., Uraushihara, K., Iiyama, R., Totsuka, T., Takeda, K., Akira, S., and Watanabe, M. (2005). MyD88-deficient mice develop severe intestinal inflammation in dextran sodium sulfate colitis. J. Gastroenterol. *40*, 16–23.

Beutler, B. (2004). Inferences, questions and possibilities in Toll-like receptor signalling. Nature *430*, 257–263.

Bjorkbacka, H., Kunjathoor, V.V., Moore, K.J., Koehn, S., Ordija, C.M., Lee, M.A., Means, T., Halmen, K., Luster, A.D., Golenbock, D.T., and Freeman, M.W. (2004). Reduced atherosclerosis in MyD88-null mice links elevated serum cholesterol levels to activation of innate immunity signaling pathways. Nat. Med. *10*, 416–421.

Boone, D.L., Turer, E.E., Lee, E.G., Ahmad, R.C., Wheeler, M.T., Tsui, C., Hurley, P., Chien, M., Chai, S., Hitotsumatsu, O., et al. (2004). The ubiquitin-modifying enzyme A20 is required for termination of Toll-like receptor responses. Nat. Immunol. *5*, 1052–1060.

Brint, E.K., Xu, D., Liu, H., Dunne, A., McKenzie, A.N., O'Neill, L.A., and Liew, F.Y. (2004). ST2 is an inhibitor of interleukin 1 receptor and Toll-like receptor 4 signaling and maintains endotoxin tolerance. Nat. Immunol. *5*, 373–379.

Burns, K., Janssens, S., Brissoni, B., Olivos, N., Beyaert, R., and Tschopp, J. (2003). Inhibition of interleukin 1 receptor/Toll-like receptor signaling through the alternatively spliced, short form of MyD88 is due to its failure to recruit IRAK-4. J. Exp. Med. *197*, 263–268.

Chuang, T.H., and Ulevitch, R.J. (2004). Triad3A, an E3 ubiquitin-protein ligase regulating Toll-like receptors. Nat. Immunol. *5*, 495–502.

Diehl, G.E., Yue, H.H., Hsieh, K., Kuang, A.A., Ho, M., Morici, L.A., Lenz, L.L., Cado, D., Riley, L.W., and Winoto, A. (2004). TRAIL-R as a negative regulator of innate immune cell responses. Immunity *21*, 877–889.

Divanovic, S., Trompette, A., Atabani, S.F., Madan, R., Golenbock, D.T., Visintin, A., Finberg, R.W., Tarakhovsky, A., Vogel, S.N., Belkaid, Y., et al. (2005). Negative regulation of Toll-like receptor 4 signaling by the Toll-like receptor homolog RP105. Nat. Immunol. *6*, 571–578.

Eriksson, U., Ricci, R., Hunziker, L., Kurrer, M.O., Oudit, G.Y., Watts, T.H., Sonderegger, I., Bachmaier, K., Kopf, M., and Penninger, J.M.

(2003). Dendritic cell-induced autoimmune heart failure requires cooperation between adaptive and innate immunity. Nat. Med. *9*, 1484–1490.

Fiorini, E., Schmitz, I., Marissen, W.E., Osborn, S.L., Touma, M., Sasada, T., Reche, P.A., Tibaldi, E.V., Hussey, R.E., Kruisbeek, A.M., et al. (2002). Peptide-induced negative selection of thymocytes activates transcription of an NF-kappa B inhibitor. Mol. Cell *9*, 637–648.

Fukao, T., Tanabe, M., Terauchi, Y., Ota, T., Matsuda, S., Asano, T., Kadowaki, T., Takeuchi, T., and Koyasu, S. (2002). PI3K-mediated negative feedback regulation of IL-12 production in DCs. Nat. Immunol. *3*, 875–881.

Hirotani, T., Lee, P.Y., Kuwata, H., Yamamoto, M., Matsumoto, M., Kawase, I., Akira, S., and Takeda, K. (2005). The nuclear IkappaB protein IkappaBNS selectively inhibits lipopolysaccharide-induced IL-6 production in macrophages of the colonic lamina propria. J. Immunol. *174*, 3650–3657.

Honda, K., Yanai, H., Negishi, H., Asagiri, M., Sato, M., Mizutani, T., Shimada, N., Ohba, Y., Takaoka, A., Yoshida, N., and Taniguchi, T. (2005). IRF-7 is the master regulator of type-I interferon-dependent immune responses. Nature *434*, 772–777.

Iwasaki, A., and Medzhitov, R. (2004). Toll-like receptor control of the adaptive immune responses. Nat. Immunol. *5*, 987–995.

Kawai, T., Adachi, O., Ogawa, T., Takeda, K., and Akira, S. (1999). Unresponsiveness of MyD88-deficient mice to endotoxin. Immunity *11*, 115–122.

Kinjyo, I., Hanada, T., Inagaki-Ohara, K., Mori, H., Aki, D., Ohishi, M., Yoshida, H., Kubo, M., and Yoshimura, A. (2002). SOCS1/JAB is a negative regulator of LPS-induced macrophage activation. Immunity *17*, 583–591.

Kisielow, P., Bluthmann, H., Staerz, U.D., Steinmetz, M., and von Boehmer, H. (1988). Tolerance in T-cell-receptor transgenic mice involves deletion of nonmature CD4+8+ thymocytes. Nature *333*, 742–746.

Kitajima, S., Takuma, S., and Morimoto, M. (1999). Changes in colonic mucosal permeability in mouse colitis induced with dextran sulfate sodium. Exp. Anim. *48*, 137–143.

Kobayashi, K., Hernandez, L.D., Galan, J.E., Janeway, C.A., Jr., Medzhitov, R., and Flavell, R.A. (2002). IRAK-M is a negative regulator of Toll-like receptor signaling. Cell *110*, 191–202.

Kobayashi, M., Kweon, M.N., Kuwata, H., Schreiber, R.D., Kiyono, H., Takeda, K., and Akira, S. (2003). Toll-like receptor-dependent production of IL-12p40 causes chronic enterocolitis in myeloid cell-specific Stat3-deficient mice. J. Clin. Invest. *111*, 1297–1308.

Kuhn, R., Lohler, J., Rennick, D., Rajewsky, K., and Muller, W. (1993). Interleukin-10-deficient mice develop chronic enterocolitis. Cell *75*, 263–274.

Kuwata, H., Watanabe, Y., Miyoshi, H., Yamamoto, M., Kaisho, T., Takeda, K., and Akira, S. (2003). IL-10-inducible Bcl-3 negatively regulates LPS-induced TNF-alpha production in macrophages. Blood *102*, 4123–4129.

Lang, K.S., Recher, M., Junt, T., Navarini, A.A., Harris, N.L., Freigang, S., Odermatt, B., Conrad, C., Ittner, L.M., Bauer, S., et al. (2005). Toll-like receptor engagement converts T-cell autoreactivity into overt autoimmune disease. Nat. Med. *11*, 138–145.

Lawrence, T., Bebien, M., Liu, G.Y., Nizet, V., and Karin, M. (2005). IKKalpha limits macrophage NF-kappaB activation and contributes to the resolution of inflammation. Nature *434*, 1138–1143.

Leadbetter, E.A., Rifkin, I.R., Hohlbaum, A.M., Beaudette, B.C., Shlomchik, M.J., and Marshak-Rothstein, A. (2002). Chromatin-IgG complexes activate B cells by dual engagement of IgM and Toll-like receptors. Nature *416*, 603–607.

Li, Q., Lu, Q., Bottero, V., Estepa, G., Morrison, L., Mercurio, F., and Verma, I.M. (2005). Enhanced NF-(kappa)B activation and cellular function in macrophages lacking I(kappa)B kinase 1 (IKK1). Proc. Natl. Acad. Sci. USA *102*, 12425–12430.

Liew, F.Y., Xu, D., Brint, E.K., and O'Neill, L.A. (2005). Negative regulation of Toll-like receptor-mediated immune responses. Nat. Rev. Immunol. *5*, 446–458.

Michelsen, K.S., Wong, M.H., Shah, P.K., Zhang, W., Yano, J., Doherty, T.M., Akira, S., Rajavashisth, T.B., and Arditi, M. (2004). Lack of Toll-like receptor 4 or myeloid differentiation factor 88 reduces atherosclerosis and alters plaque phenotype in mice deficient in apolipoprotein E. Proc. Natl. Acad. Sci. USA *101*, 10679–10684.

Moore, K.W., de Waal Malefyt, R., Coffman, R.L., and O'Garra, A. (2001). Interleukin-10 and the interleukin-10 receptor. Annu. Rev. Immunol. *19*, 683–765.

Motoyama, M., Yamazaki, S., Eto-Kimura, A., Takeshige, K., and Muta, T. (2005). Positive and negative regulation of nuclear factor-kappaB-mediated transcription by IkappaB-zeta, an inducible nuclear protein. J. Biol. Chem. *280*, 7444–7451.

Nakagawa, R., Naka, T., Tsutsui, H., Fujimoto, M., Kimura, A., Abe, T., Seki, E., Sato, S., Takeuchi, O., Takeda, K., et al. (2002). SOCS-1 participates in negative regulation of LPS responses. Immunity *17*, 677–687.

Natoli, G., Saccani, S., Bosisio, D., and Marazzi, I. (2005). Interactions of NF-kappaB with chromatin: the art of being at the right place at the right time. Nat. Immunol. *6*, 439–445.

Pasare, C., and Medzhitov, R. (2004). Toll-dependent control mechanisms of CD4 T cell activation. Immunity *21*, 733–741.

Saccani, S., Marazzi, I., Beg, A.A., and Natoli, G. (2004). Degradation of promoter-bound p65/RelA is essential for the prompt termination of the nuclear factor kappaB response. J. Exp. Med. *200*, 107–113.

Sakaguchi, S., Negishi, H., Asagiri, M., Nakajima, C., Mizutani, T., Takaoka, A., Honda, K., and Taniguchi, T. (2003). Essential role of IRF-3 in lipopolysaccharide-induced interferon-beta gene expression and endotoxin shock. Biochem. Biophys. Res. Commun. *306*, 860–866.

Strober, W., Fuss, I.J., and Blumberg, R.S. (2002). The immunology of mucosal models of inflammation. Annu. Rev. Immunol. *20*, 495–549.

Takaoka, A., Yanai, H., Kondo, S., Duncan, G., Negishi, H., Mizutani, T., Kano, S., Honda, K., Ohba, Y., Mak, T.W., and Taniguchi, T. (2005). Integral role of IRF-5 in the gene induction programme activated by Toll-like receptors. Nature *434*, 243–249.

Takeda, K., Clausen, B.E., Kaisho, T., Tsujimura, T., Terada, N., Forster, I., and Akira, S. (1999). Enhanced Th1 activity and development of chronic enterocolitis in mice devoid of Stat3 in macrophages and neutrophils. Immunity *10*, 39–49.

Wald, D., Qin, J., Zhao, Z., Qian, Y., Naramura, M., Tian, L., Towne, J., Sims, J.E., Stark, G.R., and Li, X. (2003). SIGIRR, a negative regulator of Toll-like receptor-interleukin 1 receptor signaling. Nat. Immunol. *4*, 920–927.

Wessells, J., Baer, M., Young, H.A., Claudio, E., Brown, K., Siebenlist, U., and Johnson, P.F. (2004). BCL-3 and NF-kappaB p50 attenuate lipopolysaccharide-induced inflammatory responses in macrophages. J. Biol. Chem. *279*, 49995–50003.

Yamamoto, M., Sato, S., Hemmi, H., Hoshino, K., Kaisho, T., Sanjo, H., Takeuchi, O., Sugiyama, M., Okabe, M., Takeda, K., and Akira, S. (2003). Role of adaptor TRIF in the MyD88-independent toll-like receptor signaling pathway. Science *301*, 640–643.

Yamamoto, M., Yamazaki, S., Uematsu, S., Sato, S., Hemmi, H., Hoshino, K., Kaisho, T., Kuwata, H., Takeuchi, O., Takeshige, K., et al. (2004). Regulation of Toll/IL-1-receptor-mediated gene expression by the inducible nuclear protein IkappaBzeta. Nature *430*, 218–222.

nature immunology

Essential function for the kinase TAK1 in innate and adaptive immune responses

Shintaro Sato[1,7], Hideki Sanjo[2,3,7], Kiyoshi Takeda[4], Jun Ninomiya-Tsuji[5], Masahiro Yamamoto[2], Taro Kawai[1], Kunihiro Matsumoto[6], Osamu Takeuchi[1,2] & Shizuo Akira[1,2]

Transforming growth factor-β–activated kinase 1 (TAK1) has been linked to interleukin 1 receptor and tumor necrosis factor receptor signaling. Here we generated mouse strains with conditional expression of a *Map3k7* allele encoding part of TAK1. TAK1-deficient embryonic fibroblasts demonstrated loss of responses to interleukin 1β and tumor necrosis factor. Studies of mice with B cell–specific TAK1 deficiency showed that TAK1 was indispensable for cellular responses to Toll-like receptor ligands, CD40 and B cell receptor crosslinking. In addition, antigen-induced immune responses were considerably impaired in mice with B cell–specific TAK1 deficiency. TAK1-deficient cells failed to activate transcription factor NF-κB and mitogen-activated protein kinases in response to interleukin 1β, tumor necrosis factor and Toll-like receptor ligands. However, TAK1-deficient B cells were able to activate NF-κB but not the kinase Jnk in response to B cell receptor stimulation. These results collectively indicate that TAK1 is key in the cellular response to a variety of stimuli.

Proinflammatory cytokines such as tumor necrosis factor (TNF) and interleukin 1β (IL-1β) have a critical function in innate immune responses by eliciting inflammation[1,2]. The production of proinflammatory cytokines can be induced by various cellular stresses, including pathogenic infection. The initial recognition of invading pathogens is mediated by Toll-like receptors (TLRs), which detect distinct pathogen-associated molecular patterns[2–4]. Stimulation of cells with TLR ligands, IL-1β and TNF activates intracellular signaling pathways leading to the activation of transcription factors such as NF-κB and AP-1 (ref. 1). Activation of AP-1 is mediated by mitogen-activated protein kinases (MAPKs), including Erk, Jnk and p38. Ultimately, these transcription factors initiate expression of genes involved in inflammatory responses. It is well known that TLRs and IL-1 receptor (IL-1R) activate similar signaling pathways[3]. The cytoplasmic portions of TLRs and IL-1Rs contain the Toll–IL-1R homology domain. Ligand stimulation recruits MyD88, a Toll–IL-1R homology domain–containing adaptor protein, to the Toll–IL-1R homology domain of the receptor. Subsequently, IL-1R-associated kinases (IRAKs) are recruited and phosphorylated, and then they interact with TNF receptor (TNFR)–associated factor 6 (TRAF6)[3]. TRAF6 comprises an N-terminal RING finger domain, which has been found in a family of E3 ubiquitin ligases[5]. It has been proposed that a dimeric ubiquitin-conjugating enzyme complex composed of Ubc13 and Uev1A, together with TRAF6, can catalyze the formation of a K63-linked polyubiquitin chain[5,6]. The ubiquitination is responsible for the activation of IκB kinases (IKKs). Subsequently, phosphorylated IκB undergoes degradation by the ubiquitin-proteosome system, and NF-κB translocates into nucleus and triggers transcription of target genes[7]. Simultaneously, MAPKs are activated 'downstream' of TRAF6 by activating MAPK kinase 6 (MKK6)[8]. In the TNFR signaling pathway, ligand stimulation leads to the recruitment of adaptor proteins, including TRADD, TRAF2 and RIP1, to the receptor complex. Genetic studies have shown that TRAF2 is responsible for MAPK activation, whereas RIP1 is required for NF-κB activation[1,4].

Transforming growth factor-β–activated kinase 1 (TAK1), a member of the MAPK kinase kinase (MAPKKK) family, was originally identified as a kinase involved in TGF-β signaling[9]. TAK1 is evolutionally conserved, and drosophila TAK1 is critical for antibacterial innate immunity[10]. In addition, TAK1 functions as an 'upstream' signaling molecule of NF-κB and MAPKs in IL-1R signaling pathways. Furthermore, TAK1 is activated by TNF, bacterial lipopolysaccharide (LPS) and latent membrane protein 1 from Epstein-Barr virus[11–13]. Activated TAK1 is recruited to TRAF6 and TRAF2 complexes in response to IL-1R and TNFR stimulation, respectively. A point mutation in the gene encoding TAK1 altering its ATP-binding domain abolishes both its kinase activity and its ability to activate IKKs and MAPKs[8]. TAK1 forms a complex with its association partners, TAB1, TAB2 and TAB3 (refs. 14–17). It has been proposed that TRAF6-mediated K63-linked

[1]Akira Innate Immunity Project, Exploratory Research for Advanced Technology, Japan Science and Technology Agency and [2]Department of Host Defense, Research Institute for Microbial Diseases, Osaka University, Suita, Osaka 565-0871, Japan. [3]Lymphocyte Differentiation, RIKEN Research Center for Allergy and Immunology, Yokohama, Kanagawa 230-0045, Japan. [4]Department of Molecular Genetics, Medical Institute of Bioregulation, Kyushu University, Fukuoka 812-8582, Japan. [5]Department of Environmental and Molecular Toxicology, North Carolina State University, Raleigh, North Carolina 27695-7633, USA. [6]Department of Molecular Biology, Graduate School of Science, Nagoya University, Nagoya, 464-8602, Japan. [7]These authors contributed equally to this work. Correspondence should be addressed to S.A. (sakira@biken.osaka-u.ac.jp).

Received 4 April; accepted 10 August; published online 25 September 2005; doi:10.1038/ni1255

polyubiquitination is required for the activation of TAK1. Activated TAK1 complex phosphorylates IKKs and MKK6, which activate NF-κB and MAPKs, respectively. *In vitro* studies have shown that expression of TAK1 together with TAB1 enhances activation of a NF-κB reporter gene[8]. Reciprocally, 'knockdown' of *Map3k7*, the gene encoding TAK1, in HeLa cells by RNA interference results in abrogation of IL-1β- and TNF-induced NF-κB activation[11].

The function of TAB1 and TAB2 has been assessed by examination of mouse models lacking genes encoding these proteins. Analysis of TAB2-deficient mice has shown that TAB2 is dispensable for IL-1R signaling[18]. Studies of TAB1-deficient mice have shown that TAB1 is involved in TGF-β signaling[19]. However, the function of TAB1 in IL-1R signaling *in vivo* has not been described. Therefore, it is still unclear whether TAK1-binding proteins are essential for TAK1 activation or if the TAK1 complex itself is dispensable for NF-κB and MAPK signaling *in vivo*. Although the function of TAK1 in drosophila innate immune response has been studied extensively[10], its involvement in the mammalian TLR system is not well understood.

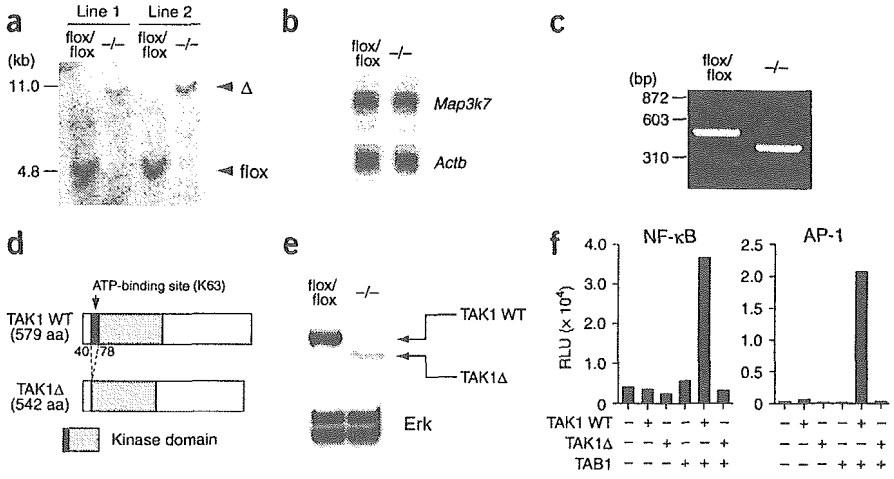

Figure 1 Establishment of *Map3k7*$^{-/-}$ MEFs. (**a**) Southern blot analysis of genomic DNA from *Map3k7*$^{-/-}$ (−/−) and control *Map3k7*$^{flox/flox}$ (flox/flox) MEFs, after digestion with *Xba*I and *Eco*RI (probe, **Supplementary Fig. 1** online). Right and left margins, positions of 11.0-kb floxed and 4.8-kb Δ fragments. (**b**) RNA blot analysis of total RNA prepared from *Map3k7*$^{-/-}$ and *Map3k7*$^{flox/flox}$ MEFs. The 5′ ends of *Map3k7* and *Actb* (encoding β-actin) cDNA fragments were used as probes. (**c**) RT-PCR analysis of total RNA from MEFs, using primers amplifying the encoding region of exons 1–3. (**d**) Predicted structure of TAK1Δ, which lacks the ATP-binding site (arrow) required for kinase activity. WT, wild-type; aa, amino acids. (**e**) Immunoblot analysis of lysates of *Map3k7*$^{-/-}$ and *Map3k7*$^{flox/flox}$ MEFs (antibodies, right margin). (**f**) NF-κB- or AP-1-dependent reporter assay. HEK293 cells were transiently transfected with plasmids (below graphs) plus an NF-κB-dependent (left) or an AP-1-dependent (right) luciferase reporter plasmid. Then, 36 h after transfection, luciferase activity (RLU, relative light units) in whole-cell lysates was measured. Data are representative of three independent experiments.

Here we have examined the function of TAK1 *in vivo* by gene targeting using the Cre-*lox*P system. *Map3k7* deficiency in the germline resulted in early embryonic death. Therefore, we generated TAK1-deficient (*Map3k7*$^{-/-}$) mouse embryonic fibroblasts (MEFs) by *in vitro* introduction of Cre in MEFs homozygous for *lox*P-flanked (floxed) *Map3k7* alleles (*Map3k7*$^{flox/flox}$). First we examined the function of TAK1 in IL-1R and TNF signaling using TAK1-deficient MEFs and found that TAK1 was required for IL-1β- and TNF-induced NF-κB and Jnk activation as well as cytokine production. Next we analyzed TLR- and B cell receptor (BCR)–mediated signaling using B cells as a model. B cell–specific deletion of TAK1 resulted in considerably impaired B cell activation in response to various stimuli, including nonmethylated CpG DNA (a ligand for TLR9), polyinosine-polycytidylic acid (poly(I:C); a ligand for TLR3), LPS (a ligand for TLR4), CD40 and BCR crosslinking. Furthermore, LPS and CpG DNA failed to activate Jnk and NF-κB in TAK1-deficient B cells, indicating that TAK1 is essential for activating these signaling pathways. Notably, although BCR crosslinking on TAK1-deficient B cells also demonstrated defective Jnk activation, activation of NF-κB as well as expression of NF-κB target genes was comparable to that of wild-type cells. Our conditional TAK1-deficient mouse model therefore shows that TAK1 is essential for TLR, IL-1R, TNFR and BCR cellular responses and signaling pathways leading to the activation of Jnk and/or NF-κB.

RESULTS

Map3k7$^{-/-}$ mice die early *in utero*

To investigate the function of TAK1 *in vivo*, we generated mice with conditional deletion of a *Map3k7* allele. We constructed a gene-targeting vector by placing *lox*P sites flanking exon 2 of mouse *Map3k7*, which encodes a part of the kinase domain of TAK1, including its ATP-binding site (Lys63), and a floxed neomycin-resistance gene into an intron 1 of *Map3k7* (**Supplementary Fig. 1** online). To generate mice heterozygous for deletion of this *Map3k7* allele (*Map3k7*$^{+/-}$ mice), we mated mice with one floxed allele and one wild-type allele (*Map3k7*$^{flox/+}$ mice) with a mice of a transgenic line expressing Cre in germ cells. We confirmed deletion of *Map3k7* in the germline by Southern blot analysis (**Supplementary Fig. 1** online). Of about 90 newborn pups obtained by intercrossing *Map3k7*$^{+/-}$ mice, we obtained no *Map3k7*$^{-/-}$ mice, indicating that the TAK1 deficiency is embryonically lethal (**Supplementary Fig. 1** online). Although we identified *Map3k7*$^{-/-}$ embryos on embryonic day 9.5 (E9.5) in normal mendelian ratios, we found no *Map3k7*$^{-/-}$ fetuses in decidua containing normal fetuses after E10.5 (**Supplementary Fig. 1** online).

Establishment of *Map3k7*$^{-/-}$ MEFs

As *Map3k7*$^{-/-}$ MEFs obtained from E9.5 embryos failed to grow, we prepared MEFs from *Map3k7*$^{flox/flox}$ mice. To generate TAK1-deficient MEFs, we excised the floxed genomic fragment by retroviral expression of Cre protein together with green fluorescent protein (GFP). We sorted GFP$^+$ cells by flow cytometry. Southern blot analysis showed that complete conversion of the floxed allele to the deleted (Δ) allele was achieved in GFP$^+$ cells from two lines of *Map3k7*$^{-/-}$ MEFs (**Fig. 1a**). However, we detected *Map3k7* transcripts in *Map3k7*$^{-/-}$ MEFs with same migration and intensity as that of *Map3k7*$^{flox/flox}$ MEFs (**Fig. 1b**). RT-PCR analysis using primers to amplify the region of exons 1–3 showed a product with faster migration in *Map3k7*$^{-/-}$ cells (**Fig. 1c**). Nucleotide sequence analysis of the product showed that the deletion of exon 2 from TAK1 cDNA was in-frame, indicating that Cre-mediated deletion led to the production of an altered TAK1 (TAK1Δ; **Fig. 1d**). Immunoblot analysis showed weak expression of TAK1Δ in *Map3k7*$^{-/-}$ cells (**Fig. 1e**). To confirm that TAK1Δ lacked

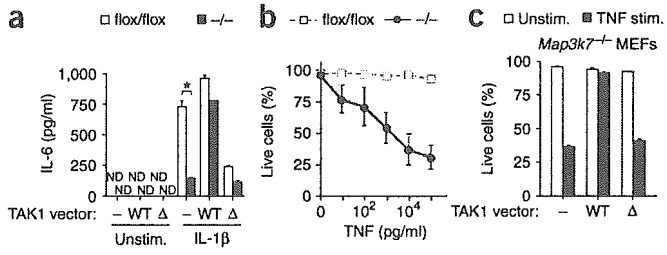

Figure 2 Impaired responses to IL-1β and TNF in *Map3k7*$^{-/-}$ MEFs. (**a**) IL-6 production by MEFs. Control *Map3k7*$^{flox/flox}$ and *Map3k7*$^{-/-}$ MEFs were transfected with empty (−), wild-type TAK1 (WT) or TAK1Δ (Δ) plasmid, and then were stimulated for 24 h with 10 ng/ml of IL-1β. IL-6 in the culture medium was measured by ELISA. Data are mean ± s.d. of triplicate samples of one representative from three independent experiments. *, $P < 0.005$, versus TAK1-deficient cells (Student's *t*-test). ND, not detected. (**b**) Viability of control and *Map3k7*$^{-/-}$ MEFs treated for 24 h with various concentrations of TNF (horizontal axis), assessed by annexin V–indocarbocyanine staining. Three independent experiments were done in triplicate. Data are mean ± s.d. percentage of viable cells after treatment relative to untreated control. (**c**) Viability of control and *Map3k7*$^{-/-}$ MEFs left untransfected or transfected with wild-type or mutated TAK1 and were left unstimulated (Unstim.) or were stimulated for 24 h with 10 ng/ml of TNF (TNF stim.). Data represent mean ± s.d. for percentage of viable cells after treatment relative to untreated control.

the ability to activate NF-κB and AP-1, we did a reporter assay. Overexpression of wild-type TAK1, but not TAK1Δ, together with TAB1 in human embryonic kidney 293 (HEK293) cells activated NF-κB and AP-1, indicating that TAK1Δ was nonfunctional because it lacked an ATP-binding site (**Fig. 1f**).

TAK1 is required for IL-1β and TNF responsiveness

We first examined responses to IL-1β and TNF. We stimulated *Map3k7*$^{-/-}$ and control *Map3k7*$^{flox/flox}$ MEFs with IL-1β and measured IL-6 production by enzyme-linked immunosorbent assay (ELISA). Production of IL-6 was impaired considerably in *Map3k7*$^{-/-}$ MEFs compared with that in control cells (**Fig. 2a**). Moreover, re-expression of wild-type TAK1 but not TAK1Δ in *Map3k7*$^{-/-}$ MEFs restored IL-6 production in response to IL-1β.

As NF-κB activation is required for survival of MEFs after exposure to TNF, we next compared the viability of TNF-stimulated cells. TNF stimulation induced cell death in *Map3k7*$^{-/-}$ MEFs in a dose-dependent way (**Fig. 2b**). In contrast, *Map3k7*$^{flox/flox}$ MEFs were viable after TNF stimulation. The TNF-induced cell death noted in *Map3k7*$^{-/-}$ MEFs was circumvented by expression of wild-type TAK1 but not TAK1Δ (**Fig. 2c**). These results indicate that TAK1 is required for IL-1β- and TNF-mediated cellular responses.

We further examined the activation of signaling molecules. In both *Map3k7*$^{flox/flox}$ and *Map3k7*$^{-/-}$ MEFs, IRAK-1 was phosphorylated, ubiquitinated and degraded in response to IL-1β, indicating that TAK1 was not involved in IRAK-1 activation (**Fig. 3a**). Induction of NF-κB DNA binding and degradation of IκBα in response to IL-1β and TNF were compromised in *Map3k7*$^{-/-}$ MEFs (**Fig. 3b**). Furthermore, activation of Jnk and p38 in response to IL-1β and TNF in *Map3k7*$^{-/-}$ MEFs was also impaired (**Fig. 3c**). Thus, TAK1 was required for NF-κB, Jnk and p38 activation in response to IL-1β and TNF in MEF cells.

Generation of mice with B cell–specific TAK1 deficiency

Although the involvement of TAK1 in the IL-1β signaling has been studied extensively, its involvement in the TLR signaling pathway is less understood. Because B cells express various TLRs and respond to their ligands to proliferate, we generated mice with B cell–specific TAK1 deficiency by breeding *Map3k7*$^{flox/-}$ mice with mice carrying the *Cre* transgene under control of the *Cd19* promoter (*Cd19*$^{Cre/+}$). Southern blot analysis showed almost complete Cre-mediated deletion of *Map3k7* in B cells from *Cd19*$^{Cre/+}$*Map3k7*$^{flox/-}$ mice (**Supplementary Fig. 2** online). We also checked deletion of TAK1 in purified B cells by immunoblot analysis and confirmed that the expression of wild-type TAK1 was considerably reduced in B cells from *Cd19*$^{Cre/+}$*Map3k7*$^{flox/-}$ mice (**Supplementary Fig. 2** online).

TAK1 deficiency impairs B-1 B cell development

We investigated whether B cell–specific TAK1 deficiency affected lymphopoiesis. The population of B cell precursors in the bone marrow was comparable in *Cd19*$^{Cre/+}$*Map3k7*$^{flox/+}$ and *Cd19*$^{Cre/+}$*Map3k7*$^{flox/-}$ mice (**Fig. 4a**). The ratio of B cells to T cells, the expression of surface immunoglobulin M (IgM) and IgD on mature splenic B cells and the numbers of marginal zone B cells (IgM$^+$CD23$^-$CD21$^+$) were also comparable for *Cd19*$^{Cre/+}$*Map3k7*$^{flox/+}$ and *Cd19*$^{Cre/+}$*Map3k7*$^{flox/-}$ splenocyte samples (**Fig. 4b**). However, the B220$^+$CD5$^+$ B-1 B cell population was reduced in the peritoneal cavities of *Cd19*$^{Cre/+}$*Map3k7*$^{flox/-}$ mice (**Fig. 4c**). These results indicate that TAK1 was required for the development of B-1 B cells but not of splenic follicular and marginal zone B cells.

TAK1 is required for the TLR signaling in B cells

B cells become active and progress through the cell cycle in response to TLR ligands such as LPS, CpG DNA and poly(I:C). Although *Cd19*$^{Cre/+}$*Map3k7*$^{flox/+}$ B cells proliferated in response to all TLR

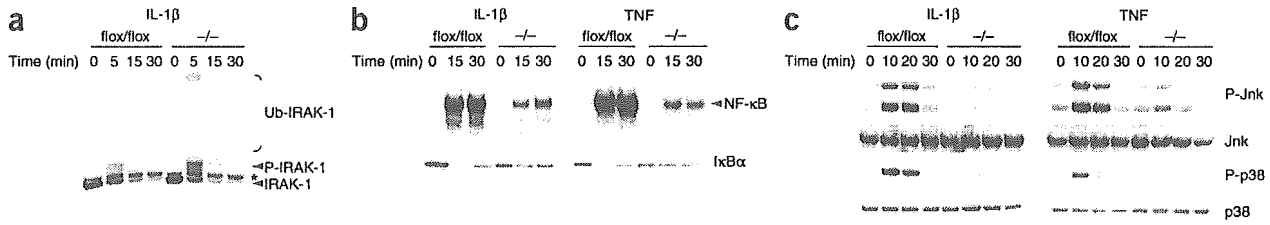

Figure 3 Impaired activation of NF-κB and MAPKs in response to IL-1β and TNF in TAK1-deficient cells. (**a**) Immunoblot of IRAK-1 in whole-cell lysates of control and *Map3k7*$^{-/-}$ MEFs left untreated or treated with 10 ng/ml of IL-1β (time, above lanes). Ub-, ubiquitinated; P-, phosphorylated; *, nonspecific band. (**b**) Control and *Map3k7*$^{-/-}$ MEFs were treated with IL-1β (10 ng/ml) or TNF (10 ng/ml) for various times (above lanes). The NF-κB DNA-binding activity in nuclear extracts was determined by EMSA (top). Degradation of IκBα whole-cell lysates was detected by immunoblot with anti-IκBα (bottom). (**c**) Phosphorylation of Jnk and p38 (P-Jnk and P-p38, respectively) in whole-cell lysates of control and *Map3k7*$^{-/-}$ MEFs treated with IL-1β (10 ng/ml) or TNF (10 ng/ml) for various times (above lanes), assessed by immunoblot with phosphorylation-specific antibodies. Jnk and p38, loading controls. All results are representative of three different experiments.

ligands tested, the proliferation of B cells from *Cd19*$^{Cre/+}$*Map3k7*$^{flox/-}$ mice was considerably impaired (**Fig. 5a**). In addition, follicular and marginal zone B-2 cells purified from *Cd19*$^{Cre/+}$*Map3k7*$^{flox/-}$ spleens had impaired proliferative responses to LPS and/or CpG DNA (**Supplementary Fig. 3** online). We also investigated cell cycle profiles by staining with bromodeoxyuridine (BrdU) and 7-amino-actinomycin D. Unlike *Cd19*$^{Cre/+}$*Map3k7*$^{flox/+}$ B cells, whose cell cycles progressed into S phase, *Cd19*$^{Cre/+}$*Map3k7*$^{flox/-}$ B cells showed impaired entry to S phase after treatment with LPS and CpG DNA (**Fig. 5b**). These results indicate that TAK1 is responsible for TLR-mediated responses in B cells.

We next examined whether TAK1 deficiency influences the viability of B cells. When control B cells were cultured *ex vivo* without mitogens, 50% of the cells spontaneously underwent apoptosis within 12 h of culture (**Fig. 5c**). Stimulation with LPS or CpG DNA prevented the execution of apoptosis in control B cells. In contrast, prevention of cell death in response to LPS or CpG DNA was impaired in *Cd19*$^{Cre/+}$*Map3k7*$^{flox/-}$ B cells. These results indicate that TAK1 is critical for TLR ligand–mediated prevention of B cell death.

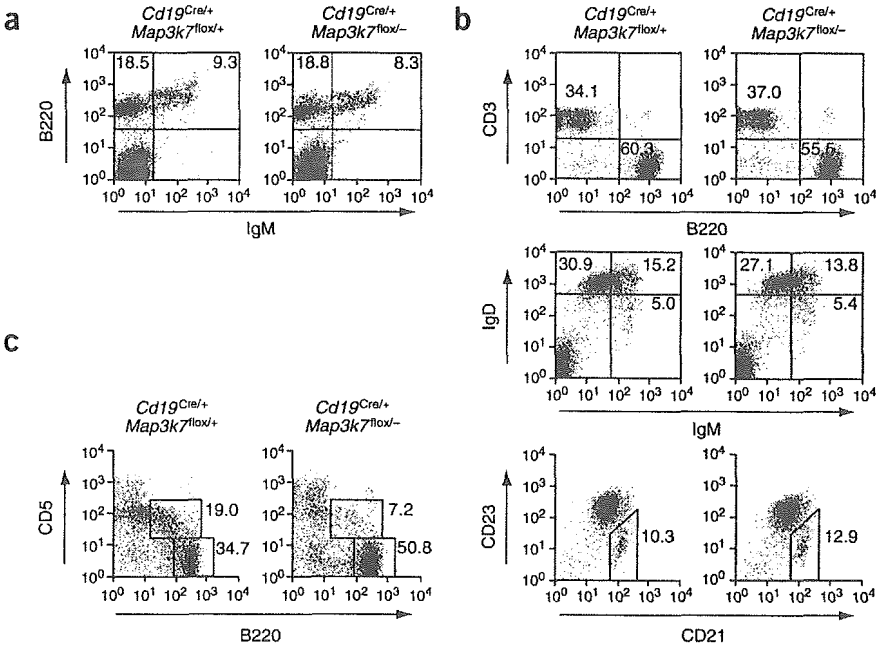

Figure 4 B cell development in *Cd19*$^{Cre/+}$*Map3k7*$^{flox/-}$ mice. Flow cytometry of B cell development in the bone marrow (**a**), splenic (**b**) and peritoneal (**c**) B cells from 8-week-old *Cd19*$^{Cre/+}$*Map3k7*$^{flox/+}$ and *Cd19*$^{Cre/+}$*Map3k7*$^{flox/-}$ mice. Numbers in the quadrants or beside boxed areas indicate the percentage of positive cells in that region. Results are representative of four different experiments.

We further analyzed the upregulation of surface activation markers in response to TLR stimuli. In accordance with defects in cell proliferation and apoptosis inhibition, *Cd19*$^{Cre/+}$*Map3k7*$^{flox/-}$ B cells stimulated with LPS or CpG DNA showed impaired upregulation of cell surface CD69 and CD86 expression (**Fig. 5d**). It has been reported that CpG DNA induces IL-6 production from human naive B cells[20]. In mouse splenic B cells, IL-6 was produced in response to CpG DNA and LPS (**Fig. 5e**). However, IL-6 production by *Cd19*$^{Cre/+}$*Map3k7*$^{flox/-}$ B cells in response to either LPS or CpG DNA was less than that of control *Cd19*$^{Cre/+}$*Map3k7*$^{flox/+}$ B cells.

We also assessed TLR-induced activation of signaling pathways in TAK1-deficient B cells. In *Cd19*$^{Cre/+}$*Map3k7*$^{flox/+}$ B cells, stimulation with LPS or CpG DNA resulted in degradation of IκBα and activation of NF-κB DNA-binding activity (**Fig. 5f,g**). In contrast, IκBα degradation and NF-κB DNA-binding activity in response to LPS and CpG DNA were reduced considerably in *Cd19*$^{Cre/+}$*Map3k7*$^{flox/-}$ B cells. In addition, activation of Jnk, p38 and Erk was impaired in LPS- and CpG DNA–stimulated *Cd19*$^{Cre/+}$*Map3k7*$^{flox/-}$ B cells (**Fig. 5h**). These findings indicate that TAK1 is critical for TLR-mediated B cell activation and signaling.

Requirement for TAK1 for activation of BCR signaling

BCR signaling also activates NF-κB and MAPKs, leading to B cell activation. Crosslinking of BCRs induces activation of tyrosine kinases, an increase in intracellular calcium and activation of protein kinase C-β[21]. A complex of the signaling molecules CARD11 (also known as CARMA1), Bcl10 and MALT1 (also known as paracaspase) then transduces signals to NF-κB and MAPKs downstream of protein kinase C-β[22]. It has also been proposed that TAK1 is involved in T cell receptor signaling downstream of TRAF6 to activate NF-κB[23]. However, the function of TAK1 in BCR signaling is unknown. We therefore analyzed activation of TAK1-deficient B cells in response to BCR crosslinking. Inactivation of TAK1 considerably impaired the proliferation of purified B cells in response to BCR and CD40 stimulation, similar to their response to TLR ligands, indicating that TAK1 is involved in the signaling pathways used by BCRs and CD40 (**Fig. 6a** and **Supplementary Fig. 3** online). Furthermore, *Cd19*$^{Cre/+}$*Map3k7*$^{flox/-}$ B cells showed impaired entry to S phase and impaired enhancement of cell survival after BCR crosslinking compared with that of control *Cd19*$^{Cre/+}$*Map3k7*$^{flox/+}$ B cells (**Fig. 6b,c**). In contrast, BCR stimulation induced almost similar upregulation of CD69 and CD86 in control and *Cd19*$^{Cre/+}$*Map3k7*$^{flox/-}$ B cells (**Fig. 6d**).

We next examined the activation of BCR-mediated signaling pathways in further detail. Tyrosine phosphorylation of cytoplasmic proteins in response to BCR stimulation was not altered in *Cd19*$^{Cre/+}$*Map3k7*$^{flox/-}$ B cells (**Fig. 6e**). Unexpectedly, BCR-mediated activation of NF-κB was not impaired in TAK1-deficient B cells (**Fig. 6f,g**). Among MAPKs, activation of Jnk but not p38 or Erk was considerably impaired (**Fig. 6h**). These data demonstrate that the requirement for TAK1 in NF-κB activation differs depending on the stimuli, whereas TAK1 functions as an essential activator of Jnk in response to a variety of stimuli.

To further elucidate how TAK1 regulates BCR-mediated proliferative responses, we investigated BCR-induced gene expression profiles by microarray analysis. The BCR-mediated expression of genes involved in cell cycling and survival was not impaired in *Cd19*$^{Cre/+}$*Map3k7*$^{flox/-}$ B cells (**Supplementary Table 1** online). The upregulation of cyclin D2 protein as well as mRNA was comparable in BCR-stimulated control and TAK1-deficient B cells (**Supplementary Fig. 4** and **Supplementary Table 1** online). However, the downregulation of p27^{Kip1} expression was impaired in *Cd19*$^{Cre/+}$*Map3k7*$^{flox/-}$ B cells, suggesting that G1-S progression was impaired at the level of p27 expression (**Supplementary Fig. 4** online).

Bcl10 and CARD11 are crucial for BCR-induced Jnk and NF-κB activation. In contrast, MALT1 is required for the activation of NF-κB